

Aus der Neurologischen Klinik und Poliklinik
der Ludwig – Maximilians – Universität München

Direktorin: Prof. Dr. med. Marianne Dieterich

Neuropathology of Chorea-acanthocytosis

Dissertation

zum Erwerb des Doktorgrades der Medizin
an der Medizinischen Fakultät der
Ludwig – Maximilians – Universität zu München

vorgelegt von

Jia Liu

aus

Tianjin (China)

2014

Mit Genehmigung der Medizinischen Fakultät
der Universität München

Berichterstatter: Prof. Dr. med. Adrian Danek

Mitberichterstatter: Priv. Doz. Dr. Rupert Egensperger

Priv. Doz. Dr. Siegfried Knösel

Mitbetreuung durch den

promovierten Mitarbeiter: Dr. med. Benedikt Bader

Dr. med. Thomas Arzberger

Dekan: Prof. Dr. med. Dr. h.c. M. Reiser, FACR, FRCR

Tag der mündlichen Prüfung: 10.04.2014

Eidesstattliche Versicherung

Liu Jia

Name, Vorname

Ich erkläre hiermit an Eides statt,
dass ich die vorliegende Dissertation mit dem Thema
Neuropathology of Chorea-acanthocytosis

selbständig verfasst, mich außer der angegebenen keiner weiteren Hilfsmittel bedient und alle Erkenntnisse, die aus dem Schrifttum ganz oder annähernd übernommen sind, als solche kenntlich gemacht und nach ihrer Herkunft unter Bezeichnung der Fundstelle einzeln nachgewiesen habe.

Ich erkläre des Weiteren, dass die hier vorgelegte Dissertation nicht in gleicher oder in ähnlicher Form bei einer anderen Stelle zur Erlangung eines akademischen Grades eingereicht wurde.

Munich, 11.04.2014

Ort, Datum

Unterschrift Doktorandin/Doktorand

Contents

| | |
|---|----|
| 1 Introduction | 1 |
| 1.1 Epidemiology | 1 |
| 1.2 Genetics | 1 |
| 1.3 Pathology..... | 2 |
| 1.4 Clinical Features | 3 |
| 1.5 Diagnosis..... | 4 |
| 1.6 Treatments..... | 5 |
| 2 Aims of Study | 6 |
| 3 Materials and Methods..... | 7 |
| 3.1 Patients..... | 7 |
| 3.2 Immunoblot..... | 11 |
| 3.3 Stains of slices | 11 |
| 3.4 Image analyses..... | 12 |
| 3.5 Stereological analyses | 14 |
| 3.6 Statistical analysis..... | 15 |
| 3.7 Literature reviews | 15 |
| 4 Results | 17 |
| 4.1 ChAc pathology in striatum | 17 |
| 4.2 ChAc pathology in hippocampus | 21 |
| 4.3 Specific accumulations in ChAc brain | 25 |
| 4.4 Stereology of ChAc brain | 27 |
| 4.5 Normal distribution of Chorein in the brain and peripheral organs | 35 |
| 4.6 ChAc pathology in muscle | 37 |
| 4.7 ChAc pathology in nerve..... | 42 |
| 4.8 Epidemiology of NA in China | 43 |

| | |
|--|----|
| 5 Discussion | 46 |
| 5.1 ChAc pathology in striatum | 46 |
| 5.2 ChAc pathology in hippocampus | 47 |
| 5.3 Specific accumulations in ChAc brain | 48 |
| 5.4 Stereology of ChAc brain | 49 |
| 5.5 Chorein distributions in human tissues | 52 |
| 5.6 ChAc pathology in muscle and nerve | 53 |
| 5.7 Epidemiology of NA in China | 54 |
| 6 Outlook | 57 |
| 7 Summary | 59 |
| 8 Zusammenfassung | 61 |
| 9 Appendix | 63 |
| 10 Abbreviations | 65 |
| 11 References | 67 |
| 12 Acknowledgement..... | 80 |

1 Introduction

The confirmed inheritance of Chorea-acanthocytosis (ChAc) is autosomal recessive (Danek et al. 2012; Walker et al. 2012), and the most common phenotype of neuroacanthocytosis (NA) syndromes. The mean onset of ChAc patients is in the third decade. It runs a progressive course leading to major disability in the next few years with reduction of life expectancy. The movement disorders are characterized by chorea, bizarre gait, orofacial dyskinesias and parkinsonism. In addition, neuropsychiatric syndromes, dementia and epilepsy are the common symptoms even at the onset (Jung et al. 2011; Walker et al. 2011).

1.1 Epidemiology

There are only hundreds of ChAc patients confirmed worldwide so far. It is likely to be substantially underestimated, because ChAc is very rare and might be not fully recognized in developing countries. For instance, the absence of reports from Africa and the former Soviet Union might be due to inaccessibility or insufficient diagnostic resources. However, as far as the experience with internationally open free diagnostic service (chorein Western blot) is concerned, the prevalence of ChAc was estimated at 1 in 10 million.

In China, the earliest report of NA can be traced back to 1980s, when the concepts of ChAc and NA have not been clearly differentiated. During the next 30 years, only sparse case reports are reported. The number of Chinese NA cases is underestimated according to the prevalence in other countries. On the other hand, NA is found to be more prevalent in Japanese. Therefore, the diagnosis and prevalence of NA syndromes in China should be carefully evaluated.

1.2 Genetics

With an autosomal recessive manner, ChAc is a *VPS13A* (formerly known as CHAC) gene related disease. Nowadays, more than 90 mutations of *VPS13A* gene have

been found (Dobson-Stone et al. 2002). Affected by mutations, 43 of the 73 exons and several introns lead to the absent or markedly reduced expression of chorein protein. The most common mutations are small deletions or insertions in exons, which cause frameshift of open reading frame of *VPS13A* and lead to premature termination codons. There are also frequent nonsense mutations and gross deletions followed by missense mutations and mutations affecting splice sites of exons.

1.3 Pathology

Chorein is found to be absent in brain tissue of ChAc patients. There are two alternative splicing variants of *VPS13A*: variant 1A (exons 1-68 and 70-73; 317kDa) and 1B (exons 1-69; 309kDa) (Velayos-Baeza et al. 2004). In Western blot of human brain tissue, two fragments of 160kDa and 94kDa probably reflect additional alternative splicing variants or posttranslational modifications (Bader et al. 2008). In mice, chorein is highly expressed in brain, testis, kidney, spleen and muscle (Kurano et al. 2007). In humans, chorein is found in erythrocyte membrane and unknown in the brain and peripheral tissues.

Previous post mortem findings in ChAc reveal atrophy of the caudate nucleus, putamen, and to a lesser extent the globus pallidus. In the striatum nonspecific but pronounced neuronal cell loss, general gliosis and microglial activation can be seen. In the striatum, spiny projection neurons are predominantly lost in ChAc. Spiny neurons mainly use gamma-aminobutyric acid (GABA) as neurotransmitter and form two populations according to neuropeptide content and projection to the globus pallidus. Those cells containing enkephalin (ENK) project primarily to the external segment of the globus pallidus (GPe), while the spiny neurons which contain substance P (SP) project mostly to the internal segment of the globus pallidus (GPi) (Haber and Elde 1981). Moreover, neuromodulators such as glutamic acid decarboxylase (GAD) and Calbindin D-28k (CALB) are important for projection

neurons in the striatum. GAD is the enzyme catalyzing formation of GABA and CALB is a calcium-binding protein and mainly present in the projection neurons (Seto-Ohshima et al. 1988).

In addition, changes in ChAc have also been described in the substantia nigra and the thalamus (Vital et al. 2002; Hardie et al. 1991), with moderate atrophy of the anterior and centromedian nuclei (Alonso et al. 1989). In contrast to Huntington's disease (HD), the corpus callosum is relatively spared in ChAc. Brain areas with no gross pathology included the subthalamic nucleus, cerebellum, pons, and medulla oblongata (Rinne et al. 1994). Muscle and nerve pathology in single case reports of ChAc suggests that muscle weakness and atrophy are mostly neurogenic alterations, rather than a pure myopathy (Limos et al. 1982; Alonso et al. 1989). Because of the low prevalence of ChAc, no study systematically evaluated the pathological changes based on a specimen series from biopsy or autopsy.

1.4 Clinical Features

The classic symptoms of ChAc can be generalized as movement disorders, seizures, and neuropsychiatric and neuromuscular symptoms. Mostly chorea is in early stage, and dystonia is common and affects the oral region and the tongue in particular. The orofacial dyskinesias include characteristic tongue protrusion, feeding dystonia, lip biting, dysarthria and dysphagia with resultant weight loss (Bader et al. 2010). The movement disorder is progressive. Parkinsonism may also occur, even as the initial presentation. The pyramidal tracts seem to be rarely involved in ChAc. Abnormalities of eye movements include impaired saccades, smooth pursuit and square-wave jerks (Gradstein et al. 2005). Seizures are observed in almost half of affected individuals and can be the initial manifestation. Seizures usually originate from temporal lobes; thus, affected individuals can present with familial temporal lobe epilepsy (Scheid et al. 2009). In cognitive deterioration, memory and executive functions, e.g. ability to

sustain concentration over time, to plan, and to change behaviour to reach a particular goal are affected, which resemble the frontal lobe syndrome. Additionally, deficits of learning and memory point to hippocampal structures as additional targets of dysfunction (Danek et al. 2005). Personality and behaviour changes emerge in about 2/3 of ChAc patients; they mainly include being apathetic, depressed, bradyphrenia, hyperactive, irritable and distractable. Moreover, obsessive-compulsive behaviors are frequent, and sometimes the onset syndrome. Common psychiatric symptoms like anxiety, aggression, autoaggression, suicide can also be seen (Walterfang et al. 2011). The myopathy is progressive and characterized by distal muscle wasting and weakness, but may remain subclinical (Saiki et al. 2007). Depression of deep tendon reflexes and vibration sense are common, resulting from an axonal neuropathy that contributes to the observed amyotrophy (Rampoldi et al. 2002).

1.5 Diagnosis

Clinical probable diagnosis mainly depends on age at disease onset, chorea, gait, orofacial and tongue protrusion dystonia, cognitive and psychiatric symptoms. Acanthocytes can be found in ChAc patient's blood with higher proportions and elevation of creatine kinase (CK) level are seen in 2/3 of ChAc patients (Danek and Walker 2005). At the same time, neuroimaging discloses atrophy of caudate nuclei with dilatation of the anterior horns, which is not specific to ChAc. Differential diagnosis includes McLeod syndrome (MLS), Huntington's disease-like 2 (HDL-2), Pantothenate kinase-associated neurodegeneration (PKAN) (also known as neurodegeneration with brain iron accumulation 1 (NBIA1)), abetalipoproteinemia, Tourette syndrome, Wilson disease, etc. Genetic analysis of *VPS13A* is the diagnostic gold standard for ChAc and the detection of chorein protein is a convenient and economic method for diagnosis. Absent or markedly reduced expression of chorein in erythrocyte membrane is highly suggestive of ChAc (Dobson-Stone et al.

2004).

1.6 Treatments

The strategy of ChAc therapy generally includes physical, pharmaceutical, and neurosurgical treatment. In drug treatment, dopamine antagonist can be used for chorea or tics and Botulinum toxin injection may be helpful to all kinds of dystonia. Antiepileptic and antipsychotic drugs are also needed according to the clinical situation. Deep brain stimulation has also been used for the therapy of ChAc (Kefalopoulou et al. 2013).

2 Aims of Study

The aims of this doctoral dissertation include the following items: 1) to know the distribution of chorein in human tissues and find out the potential role of chorein absence in the pathophysiology of ChAc 2) to explore the pathological changes in muscle and nerve tissues of ChAc and compare them with clinical clues 3) to determine the neurochemical changes in the striatum and hippocampus of ChAc, which are crucial to the pathophysiology of movement disorders and neuropsychiatric symptoms 4) to count the total number of neurons and glial cells and measure the total volume of the striatum, centromedian-parafascicular complex (CPC) and cerebral cortex by unbiased stereological procedures 5) to understand the prevalence and recognition of neuroacanthocytosis syndromes in China.

3 Materials and Methods

3.1 Patients

We collected the solid tissue samples from 10 non-ChAc controls at autopsy. Samples used for the investigation of chorein levels in non-brain tissues (cardiac muscle, bone marrow, muscle, pancreas, stomach, intestine, colon, spleen, liver, lung, kidney, ovary, testis and peripheral nerve) were derived from probands admitted to the Institute of Legal Medicine, Ludwig-Maximilians-Universität, Munich, Germany who died of reasons other than neurological or malignant disorders. A cerebrospinal fluid (CSF) sample was collected at the outpatient clinic of a 28 year old man with normal results in routine CSF analysis (albumin 21.7mg/dl; protein 41mg/dl).

Samples of muscle were collected from 10 confirmed ChAc cases, in 2 of which peripheral nerves were available (case 8 and 9). The baseline information is listed in Table 1. The tissues were derived from biceps brachii, deltoideus, gastrocnemius, psoas and quadriceps muscles by either open muscle biopsy or autopsy. Formalin-fixed and paraffin-embedded tissue was available from all cases.

Table 1 Baseline of ChAc muscles and nerves

| Case no. | Gender | Onset [age] | Biopsy/autopsy [age] | Muscle weakness | Muscle atrophy | PNS (Hyporeflexia) | DNA change | Protein change | CK | Previous report |
|----------|--------|-------------|----------------------|-----------------|----------------|--------------------|---|-------------------------------|------------------|---------------------------------------|
| 1 | M | 24 | 42 | - | UL & LL mild | + | c.883-1_892del/ c.8007del | splice-site/ p.K2669NfsX22 | Clearly elevated | Case 4 (Danek et al. 2004) |
| 2 | M | 24 | 35 | slight, distal | - | + | c.8390del/ c.9399+2_+8del | p.G2797DfsX2/ splice-site | 1470 IU/L | Case 2 (Danek et al. 2004) |
| 3 | M | 29 | 36 | - | - | + | c.3283G>C/ c.4835del | p.A1095P/ p.P1612QfsX30 | 2989 IU/L | Case 7 (Danek et al. 2004) |
| 4 | M | 26 | 36 | slight, distal | - | + | c.6059del (homozygous) | p.2020LfsX9 | Elevated | Patient 2 (Lossos et al. 2005) |
| 5 | M | 20 | 26 | n.a. | n.a. | + | c.4242+1G>T/ c.9189+8647_oGNA14:723 +897del | p.A1373FfsX7/ unknown | n.a. | Family 4 (Dobson-Stone et al. 2005) |
| 6 | M | 27 | 44 | n.a. | + | + | c.6419C>G/ c.9190del | p.S2140X/ p.V3064SfsX17 | Elevated | Case 1 (Danek et al. 2004) |
| 7 | F | 28 | 35 | n.a. | n.a. | n.a. | c.1549G>T/ c.7806 G>A | p.E517X/ splice-site | 790 IU/L | Proband 3 (Dobson-Stone et al. 2002) |
| 8 | M | 40 | 40 | LL mild | LL mild | n.a. | deletion exons 60 & 61/ c.9403C>T | unknown/ p.R3134X | 5514 IU/L | (Kageyama et al. 2007) |
| 9 | M | 25 | 47 | n.a. | n.a. | + | c.495+1G>A/ unknown | splice-site/ unknown | 2668 IU/L | Patient 13 (Dobson-Stone et al. 2004) |
| 10 | M | 28 | 44 | n.a. | + | + | n.a. | absent in Western blot | 3000 IU/L | n.a. |

F=female; LL=lower limbs; M=male; n.a.= not available; PNS=peripheral nervous system; UL = upper limbs; + =positive; - =negative

Samples of brain were collected at the Center for Neuropathology and Prion Research, Ludwig-Maximilians-Universität Munich (Brain-Net Germany) including 9 ChAc brains (5 males, 4 females), 2 HD brains (2 males) and 5 control brains (4 males, 1 female). The baseline information is provided in Table 2. The hemispheres were coronally sectioned at 0.5-1cm intervals for the regions of interest, including caudate nucleus, putamen, nucleus accumbens, globus pallidus and hippocampus. All paraffin sections were cut at a nominal thickness of 4 μm .

Table 2 Baseline of ChAc brains

| Case no. | Gender | Age of onset | Initial presentation | DNA change | Protein change | Clinical manifestation | Age at autopsy | PMI /hrs | Brain weight /g | Time of fixation /month | Previous report |
|----------|--------|--------------|----------------------|--|--------------------------------|--|----------------|----------|-----------------|-------------------------|--------------------------------------|
| ChAc 1 | M | 30 | Chorea | c.1549G>T c.7806G>A | p.E517X (splice-site mut) | Chorea, OD, Dysarthria | 32 | 119 | 1320 | n.a. | n.a. |
| ChAc 2 | F | 28 | Psychiatric symptoms | n.a. | absent in Western blot | Chorea, OD, Dysarthria, Dysphagia, CD, Seizure, SEMD, PS | 30 | 6 | 1360 | 0.5 | n.a. |
| ChAc 3 | M | 40 | Gait disturbance | deletion exons 60, 61 c.9403C>T | unknown/ p.R3134X | Chorea, Dystonia | 47 | n.a. | n.a. | n.a. | Kegeyama et al. 2007 |
| ChAc 4 | M | 32 | Seizure | c.1592del c.1592del | p.I531KfsX7 p.I531KfsX7 | Chorea, OD, Dystonia, Dysarthria, CD, Seizure, PS | 43 | 25 | 1280 | 0.5 | Burbaud et al. 2002 |
| ChAc 5 | M | 25 | Seizure | c.495+1G>A unknown | splice-site/ unknown | Hyporeflexia, Dysarthria, Parkinsonism, Seizure, PS | 47 | 68 | 1430 | 0.5 | Dobson-Stone et al. 2004, Patient 13 |
| ChAc 6 | F | 20 | Psychiatric symptoms | n.a. | absent in Western blot | Chorea, OD, Dysarthria, Dysphagia, CD, PS | 31 | 24 | 1350 | 2 | n.a. |
| ChAc 7 | F | 27 | Seizure | c.1595+1G>A c.7005G>A | (splice-site mut) p.W2335X | Chorea, OD, Dystonia, Dysarthria, SEMD, Dysphagia, Parkinsonism, CD, Seizure, PS | 57 | 11 | 1180 | 6 | Hardie et al. 1991, Case 16 |
| ChAc 8 | M | 27 | OD | c.6419C>G c.9190del | p.S2140X p.V3064SfsX17 | Chorea, OD, Dystonia, Dysarthria, SEMD, Dysphagia, Parkinsonism, CD, Seizure, PS | 53 | 58 | 1450 | 3 | Danek et al. 2004, Case 1 |
| ChAc 9 | F | 38 | Chorea | c.4592delT (Ex 38) c.4592delT (Ex 38) | p.T1530RfsX20 p.T1530RfsX20 | Chorea, OD, Dystonia, CD | 48 | n.a. | 1240 | n.a. | Foglia 2010 |

CD= cognitive decline; F= female; M= male; n.a.= not available; OD= orofacial dyskinesia; PMI= post mortem intervals; PS= Psychiatric symptoms; SEMD= Saccadic eye movement disorders

3.2 Immunoblot

Native tissue was homogenized in homogenization buffer (100mM Tris, 100mM NaCl, 10mM EDTA, 0.5% nonidet P40, 0.5% deoxycholic acid, 1 tablet protease-Inhibitor per 10ml, pH 6.9). Homogenates were cleared by centrifugation at 500 x g for 2 minutes and the supernatant containing the soluble protein fraction was used. All protein concentrations were analyzed using bicinchoninic acid protein assay. Blots were carried out using a NuPAGE pre-cast gel system. Primary antibodies anti-chor1 (polyclonal, 1:5000, gift by Antonio Velayos-Baeza, Wellcome Trust of Human Genetics, University of Oxford, UK). As secondary antibody, alkaline phosphatase-conjugated goat anti-rabbit (1:5000, Millipore, Germany) was used following standard Western blot procedures. The exact protocol of Western blot is listed in the Appendix.

3.3 Stains of slices

For peripheral organs and brains of non-ChAc cases, paraffin sections were stained with anti-VPS13A (HPA021662, polyclonal, 1:1000, Atlas Antibodies, Sweden) targeting chorein protein.

For ChAc brain sections, routine stains of hematoxylin and eosin (H&E), Klüver-Barrera (KB) and Perl's Prussian blue and immunohistochemistry of glial fibrillary acidic protein (GFAP), Cr3/43, p62, fused in sarcoma (FUS), amyloid-beta (A β), α -synuclein, AT8, and neurotransmitters such as ENK, SP, GAD and CALB were undertaken. Most immunohistochemistry stains were performed in the 'Ventana Benchmark' (Roche) autostainer. The slides were pretreated in the buffer 'cell conditioning 1' and blocked in 1% serum in PBS for 30 min. Then they were incubated in antibody directed against GFAP diluted to 1:2000 (DAKO, Z0334), Cr3/43 diluted to 1:100 (DAKO, M0775), p62 diluted to 1:100 (BD Biosciences, 610832), FUS diluted to 1:500 (Bethyl Laboratories, Inc, A300-302A-1), β -amyloid 4G8 diluted to 1:10000

(Covance, SIG-39220), α -synuclein diluted to 1:500 (BD Biosciences, 610786), AT8 diluted to 1:200 (Thermo, MN1020), ENK diluted to 1:1000 (Biotrend, ABIN98777), SP diluted to 1:50 (Biotrend, ABIN107144) or GAD diluted to 1:200 (MBL, ABIN131839). The sections were then treated with super enhancer for 20 min and polymer HRP for 30 min. Washes (2 x 5 min) in PBS followed each of the above steps. The sections were detected by 'SuperVision 2' polymer system (DCS, PD000kit) and then dehydrated and coverslipped for further evaluation. Stains of CALB were performed manually. The slides were first pretreated with citric buffer (PH 6) for 25 min, microwaved and then brought into I-block 2% with 0.2% Tween20 for 30 min. The sections were incubated in primary antibody against CALB to 1:100 (Millipore, AB1778) overnight at 4°C and in secondary antibody rabbit anti-goat IG diluted 1:400 (DAKO, Z0228) for 1 h at room temperature. Detection system is also the HRP conjugated polymer system 'SuperVision 2'.

For muscle pathology, paraffin sections were stained with H&E, Gömöri trichrome (GT) and periodic acid Schiff (PAS). Fibre typing was identified by immunohistochemistry of myosin heavy chain (MHC) slow (M8421, monoclonal, 1:1000, Sigma, Germany) and fast (M4276, monoclonal, 1:2000, Sigma, Germany) isotypes, corresponding to type 1 and type 2 fibres, respectively. Moreover, immunohistochemistry with anti-VPS13A (HPA021662, polyclonal, 1:75, Atlas Antibodies, Sweden) was also performed. For nerve pathology, paraffin sural nerve sections were stained with H&E, GT, PAS, Elastica-van Gieson (EvG). Immunohistochemistry was done for neurofilament (M0762, monoclonal, 1:500, DakoCytomation, Denmark) and myelin basic protein (MBP) (760-2658, polyclonal, purified, Ventana, USA).

3.4 Image analyses

For Western blot analyses, we calculated the integrated optical density (IOD) of the chorein band and normalized the values of IOD according to a protein concentration

of 1mg/ml. The quantitative analysis of Western blot was carried out by the software Gel-Pro Analyzer 4.0 (MediaCybernetics, USA).

For muscle pathology, fibre parameters were measured by the software Image-Pro Plus (version 6.0, MediaCybernetics, USA). In representative muscle regions, the diameter of type 1 and type 2 fibres was measured respectively. For longitudinal fibres, the diameter was defined as the maximum distance at a right angle to the fibre's longitudinal axis. The frequency of internalized nuclei was counted as the number of internalized nuclei per 100 fibres. Mean fibre diameter as well as variability, hypertrophy and atrophy coefficients were calculated for type 1 and type 2 fibres according to commonly used definitions. At least 100 fibres were measured in each sample. The cut-off values for abnormality were considered as variability coefficients above 250, and atrophy and hypertrophy coefficients above 350.

For brain pathology, the anterior striatum including caudate nucleus, putamen and nucleus accumbens was divided into dorsal striatum and ventral striatum. Differences in specific immunoreactivity for all the antibodies were compared and described. For quantitative evaluation, an Olympus microscope was used with objective x20, and 6 randomized fields were respectively selected from dorsal caudate nucleus and dorsal putamen for GFAP, ENK, SP, GAD and CALB-stains. For globus pallidus, the sections were evaluated with objective x20 for axon terminals immunoreactions of ENK in GPe, SP in Gpi, as well as GAD in both of the GPi and GPe. Each pallidal segment was divided into 6 portions, including dorsolateral, dorsomedial, midlateral, midmedial, ventrolateral and ventromedial portions. In each portion, a field (2 mm²) with the maximal density of labeled boutons was selected and the image was captured, and then measured by the software ImageJ 1.45s (NIH, USA). For hippocampus, 3 randomly selected fields were captured by an Olympus microscope with objective x20 in cornu ammonis (CA) and hilus of dentate gyrus (DG). For each

case, the number of total neurons and immunoreactive neurons were counted and the percent of positively stained neurons was calculated.

3.5 Stereological analyses

For stereology, 3 ChAc hemispheres (case 1, 8 and 9) were available. The brainstem with the cerebellum was separated from the forebrain at the level of the rostral pons, and the hemispheres were divided mediosagittally. Briefly, the hemispheres were embedded in celloidin as previously described (Heinsen et al. 2000) and cut into serial 420 μm -thick coronal sections using a sliding microtome (Polycut, Cambridge Instruments, UK). From each hemisphere, every second section was stained with gallocyanin (a Nissl stain) as previously described (Heinsen and Heinsen 1991).

Stereological analyses were performed with a stereology workstation based on a Zeiss Axioplan II microscope (Carl Zeiss MicroImaging, Thornwood, NY, USA) equipped with Plan-Neofluar objectives 2.5x (N.A. = 0.075) and 40x (N.A. = 1.30), Fluor objectives 10x (N.A. = 0.5) and 20x (N.A. = 0.75), a Microfire CCD camera (Optronics, Goleta, CA, USA), a motorized stage (Ludl Electronics, Hawthorne, NY, USA), and stereology software (Stereoinvestigator, Version 10, MBF Bioscience, Williston, VT, USA).

The regions of interest included the striatum, CPC and cerebral cortex. Delineation of striatum was performed according to established criteria (Holt et al. 1999; Lauer and Heinsen 1996). The outlines of the CPC and cerebral cortex could be clearly distinguished in the gallocyanin-stained serial sections. The volumes were calculated with Cavalieri's principle, by measuring the projection area of striatal regions on all sections and multiplying its value with the interval of the selected sections, as well as the actual thickness of sections (Kreczmanski et al. 2007). The projection area was determined by tracing the boundary of each section on video images displayed by the stereology workstation. Total cell number was evaluated with the optical fractionator

(West et al. 1991). Within the manually traced boundaries, the MBF software can generate grids and counting frames. Grids are characterized by crossing points, set apart from each other by either 1000x1000 μm (counting neurons) or 2500x2500 μm (counting of glial cells). The crossing points of the grid can be used in an identical manner like crossing points printed on transparent grids used previously for classical area or volume estimations on histological profiles (Weibel 1979). The center of a grid can be further defined as a counting frame. The counting frame for neurons was 70x70 μm , that for glial cells 15x15 μm . All cells whose nuclear boundaries or, if present, the nuclei which came into focus during constant focusing within a virtual depth of 25 μm from every counting were counted. A superficial guard zone encompassing 10 μm of the outer surface of the sections was refrained from counting. The MBF system generates counting grids and counting frames in a systematic-random fashion throughout the delineated regions. Finally, density of cells was calculated as the ratio of total cell number and the volume of this region.

3.6 Statistical analysis

Statistical analyses were performed using the statistical package for the social sciences (SPSS) for Windows, version 16.0. All tests were two-sided with $P < 0.05$ considered significant. Non-parametric test was used to identify the significance of differences in the outcomes. We assessed the bivariate correlations by Pearson correlation coefficient. For stereology, the data of HD and normal control were cited from the previous publication, in which the tissues were treated with the same way (Heinsen et al. 1994; Heinsen et al. 1996).

3.7 Literature reviews

We searched Medline (from 1949 to December 31st, 2012), China National Knowledge Infrastructure (<http://www.cnki.net>, from 1979 to December 31st, 2012) and Wanfang Data (<http://www.wanfangdata.com.cn>, from 1984 to December 31st,

2012). The search terms in English and Chinese equivalents included “neuroacanthocytosis”, “chorea-acanthocytosis”, “McLeod syndrome”, “choreoacanthocytosis”, “hereditary acanthocytosis syndrome” and “Levine-Critchley syndrome”. We also identified cases from cross-references between papers. We only included the original case reports with explicit diagnosis of NA by the original authors. The included patients had to be Chinese and diagnosed in China. We extracted and compared the information of each case with geographical origin, gender, age of onset, clinical features and laboratory findings.

4 Results

4.1 ChAc pathology in striatum

The comparison of ENK, SP, GAD and CALB immunostained images (Figure 1) in ChAc, HD and control illustrates the changes of striatal neurochemical architecture. Distinguishable decreased immunoreactivity of ENK, SP and GAD was found in ChAc and HD compared to the control, especially in dorsal caudate nucleus and dorsal putamen. They were relatively retained in the ventral part, e.g. accumbens nucleus, which was generally acknowledged as weakly immunoreactive in the normal case. In contrast, there was increased immunoreactivity of CALB in the dorsal striatum of ChAc compared to HD and control, but without obvious changes in the ventral striatum.

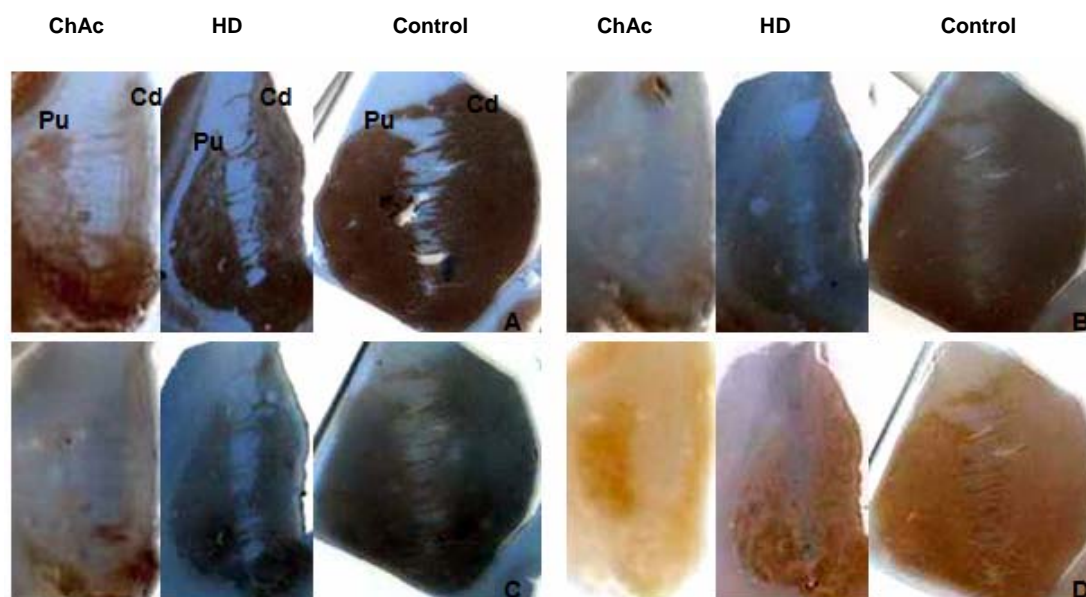
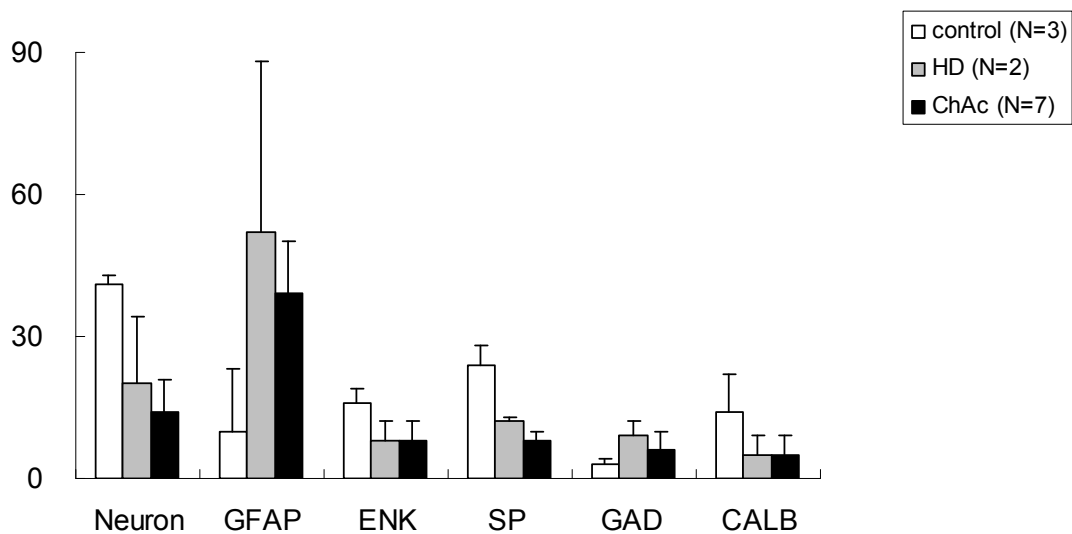


Figure 1 Images of immunostained striatum of GAD (A), SP (B), ENK (C) and CALB (D) illustrated the striatal neurochemical architecture in ChAc, HD and control. There was an obvious atrophy of the caudate nucleus (Cd) and putamen (Pt) in ChAc and HD, compared to the normal control. Distinguishable decreased immunoreactivity of ENK, SP and GAD was found in ChAc and HD compared to the control, especially in dorsal caudate nucleus and dorsal putamen. In contrast, there was an increased immunoreactivity of CALB in the dorsal striatum of ChAc compared to HD and the control. Scale bars: 10mm.

The mean number of neurons, astrocytes, and immunostains was respectively

acquired and non-parametric test was used to analyse. By Mann-Whitney U test, there was a significant difference in the number of neuron between normal control and ChAc groups in dorsal caudate nucleus ($P = 0.017$) and dorsal putamen ($P = 0.024$). Concerning the number of astrocyte in normal control and ChAc groups, a significant increase was found in the dorsal caudate nucleus ($P = 0.017$) but not in the dorsal putamen ($P = 0.095$). The number of ENK immunostained neurons was decreased in dorsal caudate nucleus (Mann-Whitney U test, $P = 0.017$) and dorsal putamen (Mann-Whitney U test, $P = 0.024$) in ChAc group, compared to the control. The number of SP immunostained neurons was decreased in dorsal caudate nucleus (Mann-Whitney U test, $P = 0.017$) and dorsal putamen (Mann-Whitney U test, $P = 0.024$), compared to the control. However, the difference in the number of GAD immunostained neurons was not significant in dorsal caudate nucleus (Mann-Whitney U test, $P = 0.267$) and dorsal putamen (Mann-Whitney U test, $P = 0.095$) between ChAc and control groups, as well as the number of CALB immunostained neurons in dorsal caudate nucleus (Mann-Whitney U test, $P = 0.095$) and dorsal putamen (Mann-Whitney U test, $P = 0.167$) (Figure 2).

(A) Dorsal caudate nucleus



(B) Dorsal putamen

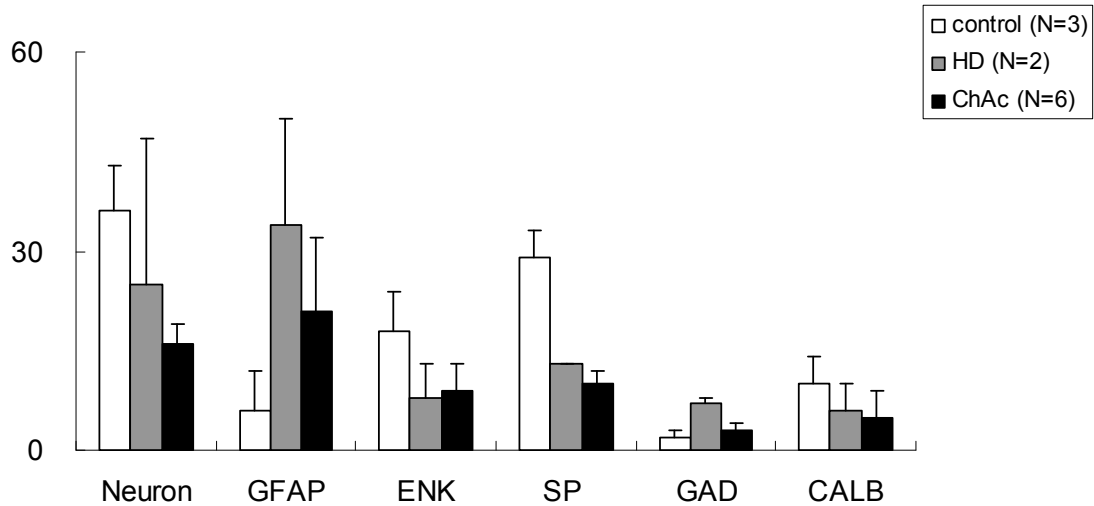
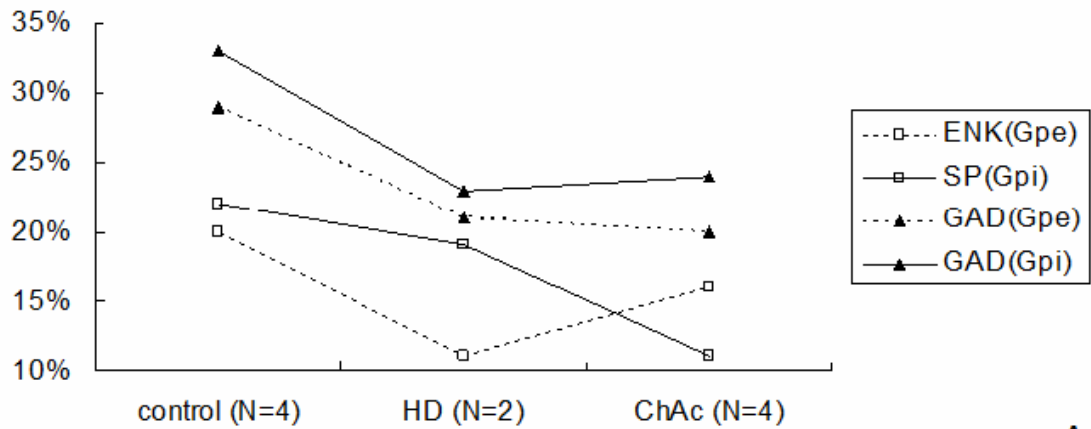


Figure 2 Qualitative neurotransmitters in dorsal striatum. By Mann-Whitney U test, significant differences of number of neuron between normal control and ChAc groups were found in dorsal caudate nucleus and dorsal putamen, while the number of astrocyte was significantly increased in ChAc group in comparison to normal control group in dorsal caudate. The number of ENK and SP immunostained neurons was respectively decreased in dorsal caudate nucleus and dorsal putamen of ChAc group compared to the control.

The mean proportion of area (in pixel units) occupied by immunoreactive ENK, GAD terminals in GPe, and SP, GAD terminals in GPi for control, HD and ChAc groups was examined and calculated. The statistical analysis showed that the reduced mean proportion of SP-positive area for ChAc group was significant (Mann-Whitney U test, $P = 0.029$) compared to the control group in GPi, while the mean proportion of ENK-positive area for ChAc group was significantly reduced (Mann-Whitney U test, $P = 0.029$) compared to the control group in GPe. Statistical differences of the proportion of GAD area were also found in GPi between ChAc and control groups (Mann-Whitney U test, $P = 0.029$), but not in GPe (Mann-Whitney U test, $P = 0.057$). In the meantime, no significant differences were found in all these proportions between ChAc and HD groups (Figure 3).



A

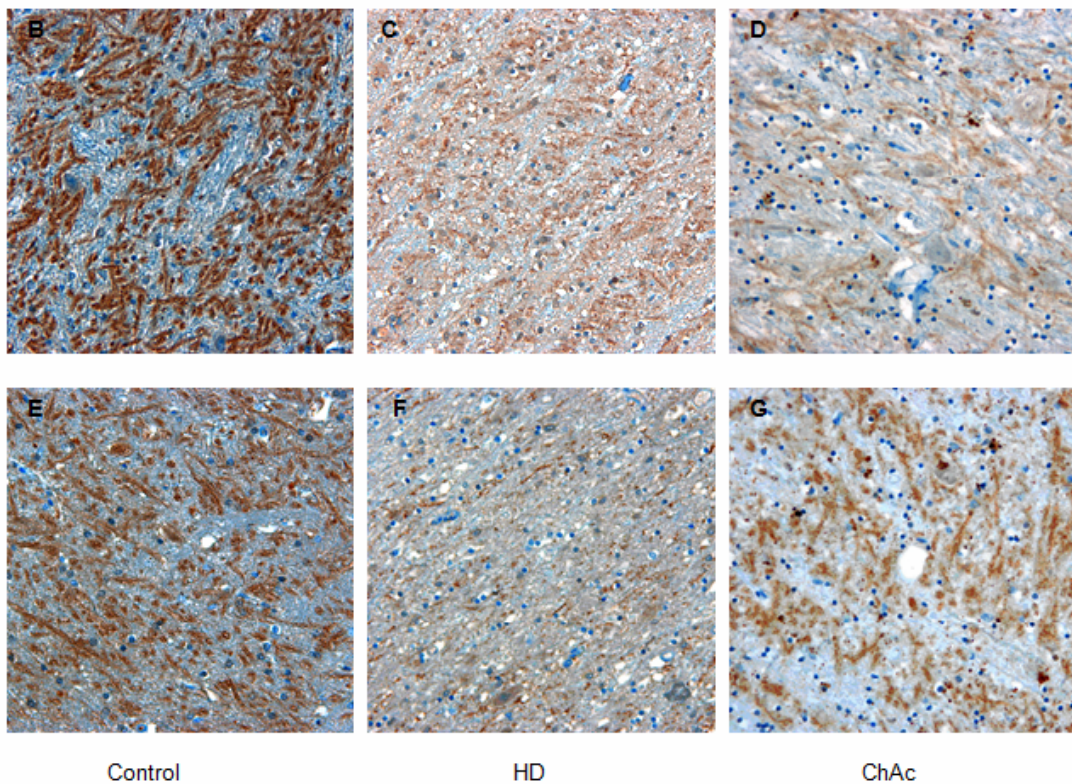


Figure 3 Qualitative neurotransmitters in globus pallidus The mean proportion of immunoreactive ENK, GAD terminals in the GPe, and SP, GAD terminals in GPi for control, HD and ChAc groups was examined and calculated (A). The statistical analysis of Mann-Whitney U test showed that the mean proportion of SP-positive area for ChAc group was significantly reduced compared to the control and HD group in the GPi, while the mean proportion of ENK-positive area for HD group was significantly reduced compared to the control group in the GPe. Statistical differences of the proportion of GAD area were also found in GPe and GPi between ChAc and control groups. In the meantime, no significant differences were found in all these proportions between ChAc and HD groups. (B-D, GPi for SP stain; E-G, GPe for ENK stain; B,E: normal control; C,F: HD; and D, G: ChAc case 5). Scale bars: 100µm.

There were positive correlations between each pair variables: the number of neurons in dorsal caudate nucleus and putamen ($r = 0.863$, $P = 0.001$); the number of astrocytes in dorsal caudate nucleus and putamen ($r = 0.858$, $P = 0.001$); the number of ENK neurons in dorsal caudate nucleus and putamen ($r = 0.835$, $P = 0.001$); the number of SP neurons in dorsal caudate nucleus and putamen ($r = 0.896$, $P < 0.001$); the number of GAD neurons in dorsal caudate nucleus and putamen ($r = 0.712$, $P = 0.014$); the number of CALB neurons in dorsal caudate nucleus and putamen ($r = 0.747$, $P = 0.008$); the number of total neurons and SP neurons in dorsal putamen ($r = 0.682$, $P = 0.021$); the number of total neurons and SP neurons in dorsal caudate nucleus ($r = 0.790$, $P = 0.002$); the number of total neuron and ENK neurons in dorsal caudate nucleus ($r = 0.672$, $P = 0.017$); the number of SP neurons and ENK neurons in dorsal caudate nucleus ($r = 0.749$, $P = 0.005$); the number of SP neurons and ENK neurons in dorsal putamen ($r = 0.676$, $P = 0.022$); the number of CALB neurons and ENK neurons in dorsal putamen ($r = 0.717$, $P = 0.013$).

4.2 ChAc pathology in hippocampus

Compared to normal controls, there was no obvious neuronal loss and gliosis in CA1 of ChAc cases based on HE and KB stains. The proportions of glial cells were gradually elevated from CA1 to CA4 in ChAc cases, which were not consistent with selective CA1 changes in HS. In addition, we did not find any abnormality in the morphology of CA neurons, glial cells and axons in HE stains. And there were normal myelinations of hippocampus in KB stains. For DG, no obvious loss or gliosis of granule cells was detected, but with dispersion of granule cells in certain ChAc cases. Immunohistochemistry illustrated the neurochemical architecture of hippocampus in normal control and ChAc (Table 3).

Table 3 Distribution of neurotransmitters in the hippocampus of control and ChAc

| Case no. | ENK | | | | SP | | | | GAD | | | | CALB | | | |
|-----------|---------|---------|---------|---------|---------|---------|---------|---------|-------|---------|--------|--------|---------|---------|---------|--|
| | CA4 | CA2/3 | CA1 | CA1 | CA4 | CA2/3 | CA1 | CA1 | CA4 | CA2/3 | CA1 | CA1 | CA4 | CA2/3 | CA1 | |
| Control 1 | G (+) | N (+) | N (++) | N (+++) | G (+++) | N (+++) | N (+++) | N (+) | G (-) | N (+) | N (+) | N (+) | G (+++) | N (+++) | N (+++) | |
| | N (+) | A (+) | A (+) | A (+++) | N (++) | A (+++) | A (+++) | A (+++) | N (+) | A (+++) | A (++) | A (++) | N (+++) | A (+++) | A (+++) | |
| Control 2 | G (+) | N (+) | N (++) | N (+++) | G (+++) | N (+++) | N (+++) | G (-) | G (-) | N (+) | N (+) | N (+) | G (+++) | N (+++) | N (+++) | |
| | N (+) | A (+) | A (+) | A (+++) | N (++) | A (+++) | A (+++) | N (+) | N (+) | A (+++) | A (++) | A (++) | N (+++) | A (+++) | A (+++) | |
| Control 3 | G (+) | N (+) | N (++) | N (+++) | G (+++) | N (+++) | N (+++) | G (-) | G (-) | N (+) | N (+) | N (+) | G (+++) | N (+++) | N (+++) | |
| | N (+) | A (+) | A (+) | A (+++) | N (++) | A (+++) | A (+++) | N (+) | N (+) | A (+++) | A (++) | A (++) | N (+++) | A (+++) | A (+++) | |
| ChAc 2 | G (++) | N (++) | N (++) | N (++) | G (++) | N (++) | N (++) | G (-) | G (-) | N (+) | N (+) | N (+) | G (++) | N (++) | N (++) | |
| | N (++) | A (-) | A (-) | A (++) | N (++) | A (++) | A (++) | N (+) | N (+) | A (+++) | A (++) | A (++) | N (++) | A (+++) | A (+++) | |
| ChAc 3 | G (++) | N (++) | N (++) | N (++) | G (+) | N (++) | N (++) | G (-) | G (-) | N (+) | N (+) | N (+) | G (+++) | N (++) | N (++) | |
| | N (++) | A (+) | A (+) | A (++) | N (++) | A (++) | A (++) | N (+) | N (+) | A (+++) | A (++) | A (++) | N (++) | A (+++) | A (++) | |
| ChAc 4 | G (++) | N (++) | N (++) | N (++) | G (+) | N (++) | N (++) | G (-) | G (-) | N (+) | N (+) | N (+) | G (++) | N (++) | N (++) | |
| | N (++) | A (-) | A (-) | A (++) | N (++) | A (++) | A (++) | N (+) | N (+) | A (+++) | A (++) | A (++) | N (++) | A (++) | A (++) | |
| ChAc 5 | G (++) | N (++) | N (++) | N (++) | G (+) | N (++) | N (++) | G (-) | G (-) | N (+) | N (+) | N (+) | G (+) | N (++) | N (++) | |
| | N (++) | A (-) | A (-) | A (++) | N (++) | A (++) | A (++) | N (+) | N (+) | A (+++) | A (++) | A (++) | N (++) | A (++) | A (++) | |
| ChAc 6 | G (+++) | N (+++) | N (+++) | N (+++) | G (+) | N (++) | N (++) | G (-) | G (-) | N (+) | N (+) | N (+) | G (++) | N (++) | N (++) | |
| | N (+++) | A (-) | A (-) | A (+) | N (++) | A (+) | A (+) | N (+) | N (+) | A (+++) | A (++) | A (++) | N (++) | A (++) | A (++) | |
| ChAc 7 | G (++) | N (++) | N (++) | N (++) | G (+) | N (++) | N (++) | G (-) | G (-) | N (+) | N (+) | N (+) | G (++) | N (++) | N (++) | |
| | N (++) | A (-) | A (-) | A (++) | N (++) | A (++) | A (++) | N (+) | N (+) | A (+++) | A (++) | A (++) | N (++) | A (++) | A (++) | |
| ChAc 8 | G (++) | N (++) | N (++) | N (++) | G (+) | N (++) | N (++) | G (-) | G (-) | N (+) | N (+) | N (+) | G (++) | N (++) | N (++) | |
| | N (++) | A (-) | A (-) | A (++) | N (++) | A (++) | A (++) | N (+) | N (+) | A (+++) | A (+) | A (+) | N (++) | A (++) | A (++) | |

- immunonegative; + occasional/weakly stained; ++ immunostained; +++ strong immunostained; G=granule cells in stratum granulosum; N=neurons in stratum pyramidale; A=axons; n.a.= not available

For ENK, there was increased expression in the neurons of the hilus of DG and CA3, but reduced in the axons of CA3 and CA1. Meanwhile, the decrease of SP immunoreactivity was found in the neurons and axons in all the hippocampus subfields. On the other hand, the density of GAD immunoreactive fibers were not obviously changed in the cornu ammonis of ChAc, as well as the CALB stained neurons and fibers. Most granule cells in the DG were CALB-positive, but the CALB stained granule cells in DG were reduced in ChAc. Moreover, granule cell loss and dispersion obviously appeared in ChAc cases with seizure. The GFAP stains in the hippocampus of ChAc suggested the astrogliosis was less affected in CA1, but more severe in the hilus of DG. In CA3, neurons were rarely stained while the surrounding fibers were markedly labeled by GFAP (Figure 4).

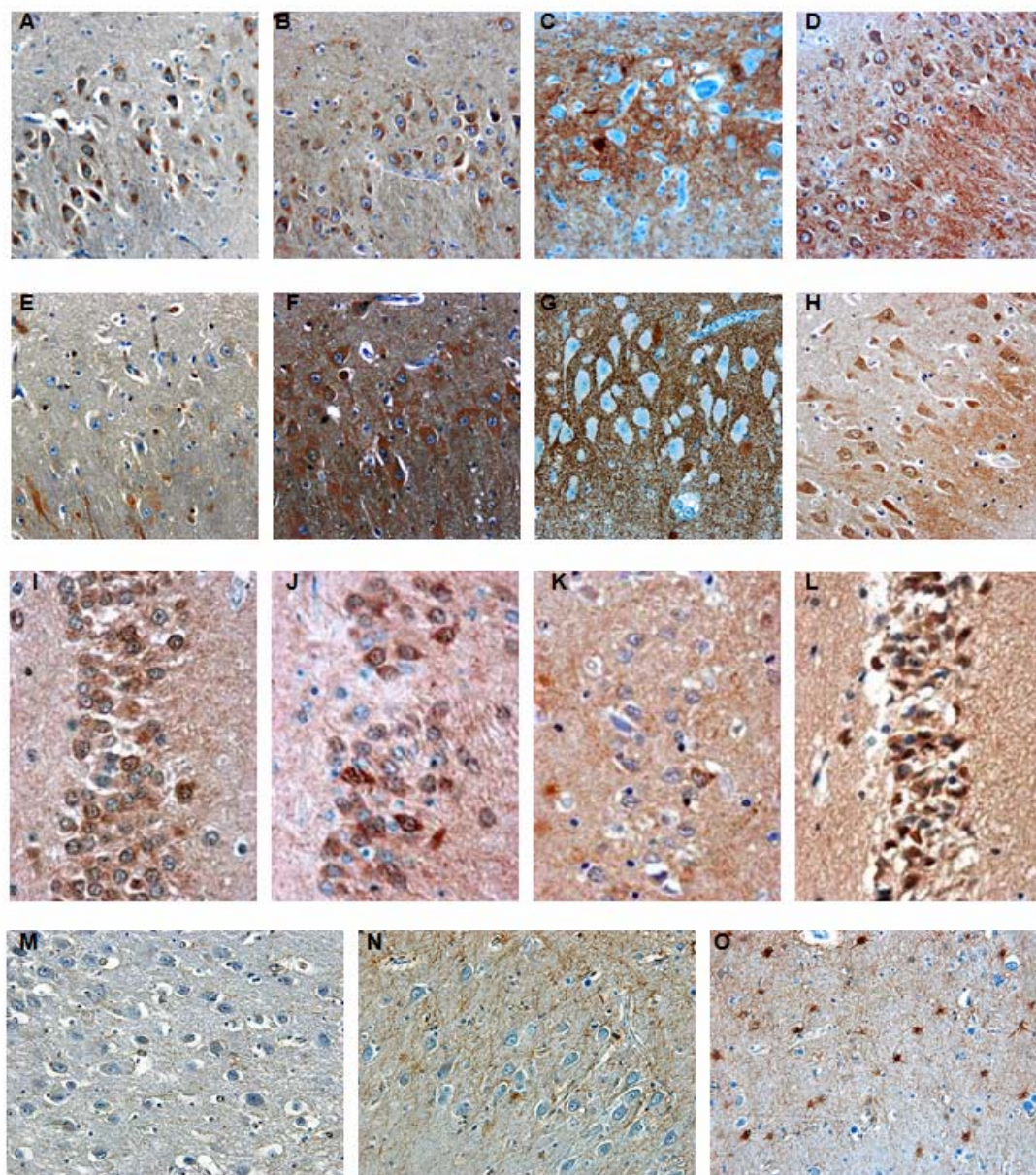


Figure 4 Neurotransmitters in hippocampus. Immunohistochemistry illustrated the comparisons of CA3 region between ChAc (case 2, A-D) and normal control (E-H). Elevated ENK was found in the neurons of ChAc (A) comparing with control (E). Decreased SP expression was distributed in the neurons and fiber throughout all the layers in ChAc (B), comparing with control (F). The density of GAD immunoreactive fibers was not changed in the stratum radiatum of ChAc (C) in comparison with the control (G), with several GAD-stained interneurons. Strong CALB stained neurons and fibers were observed in ChAc (D) and control (H) without obvious differences. Most of granule cells in DG were CALB-positive (I-L). Compared to control (I), granule cell loss and dispersion obviously appeared in ChAc case 2 (J) and case 5 (K), but did not in case 3 (L). The GFAP stains in the hippocampus of case 5 (M-O) suggested the

astrogliosis was less affected in CA1 (M), but more severe in the hilus of DG (O). In CA3, neurons were rarely stained while the surrounding fibers were markedly labeled by GFAP (N). Scale bars: 100 μ m in A-H, and M-O; 50 μ m in I-L.

We counted the number of neurons and ENK stained neurons in CA3, and calculated the proportion. There were no significant differences in the number of CA3 neurons between ChAc and control groups (Mann-Whitney U test, $P = 0.909$). Meanwhile, the significant increased percent of ENK stained neurons appeared in the ChAc group, comparing with the control group (Mann-Whitney U test, $P = 0.016$). And the same way was applied in the hilus of DG for GFAP stain. No significant differences were found in the number of neurons and the ratio of astrocytes/neurons between ChAc and control groups (Mann-Whitney U test, $P = 0.137$ and $P = 0.087$). Through the subgroup analysis, there were significant differences in the number of neurons and the ratio of astrocytes/neurons in the hilus of DG between ChAc with cognitive decline and control groups (Mann-Whitney U test, $P = 0.051$ and $P = 0.053$). The information of cognitive decline is provided in Table 2.

4.3 Specific accumulations in ChAc brain

Iron was found to deposit in the caudate nucleus, putamen and globus pallidus of ChAc cases (Figure 5, A-C). The patterns of deposition included the perivascular and parenchymal space. The affected parenchyma involved glia and axon sections. Meanwhile, nucleus accumbens and hippocampus were almost spared by iron deposition. Immunoreactivity of Cr3/43 was found in the caudate nucleus, putamen, and cornu ammonis of ChAc patients, but was relatively spared in the nucleus accumbens. For normal controls, no immunoreactivity was found in the striatum. However, there was mild immunoreactivity in the cornu ammonis (Figure 5, D-I). Concerning the α -synuclein stain, no positively-stained neurons were found in normal controls. In contrast, immunoreactivity was found in the neurons of caudate nucleus and cornu ammonis in ChAc (Figure 5, J-L). For β -amyloid 4G8, there was no classic

extracellular accumulation. But intracellular accumulations were found both in normal controls and ChAc patients without significant difference. No p62-positive inclusion was found in any case, except for sparse positive dots in the putamen of one ChAc patient (case 7). In addition, there was no immunoreactivity of AT8 in any case.

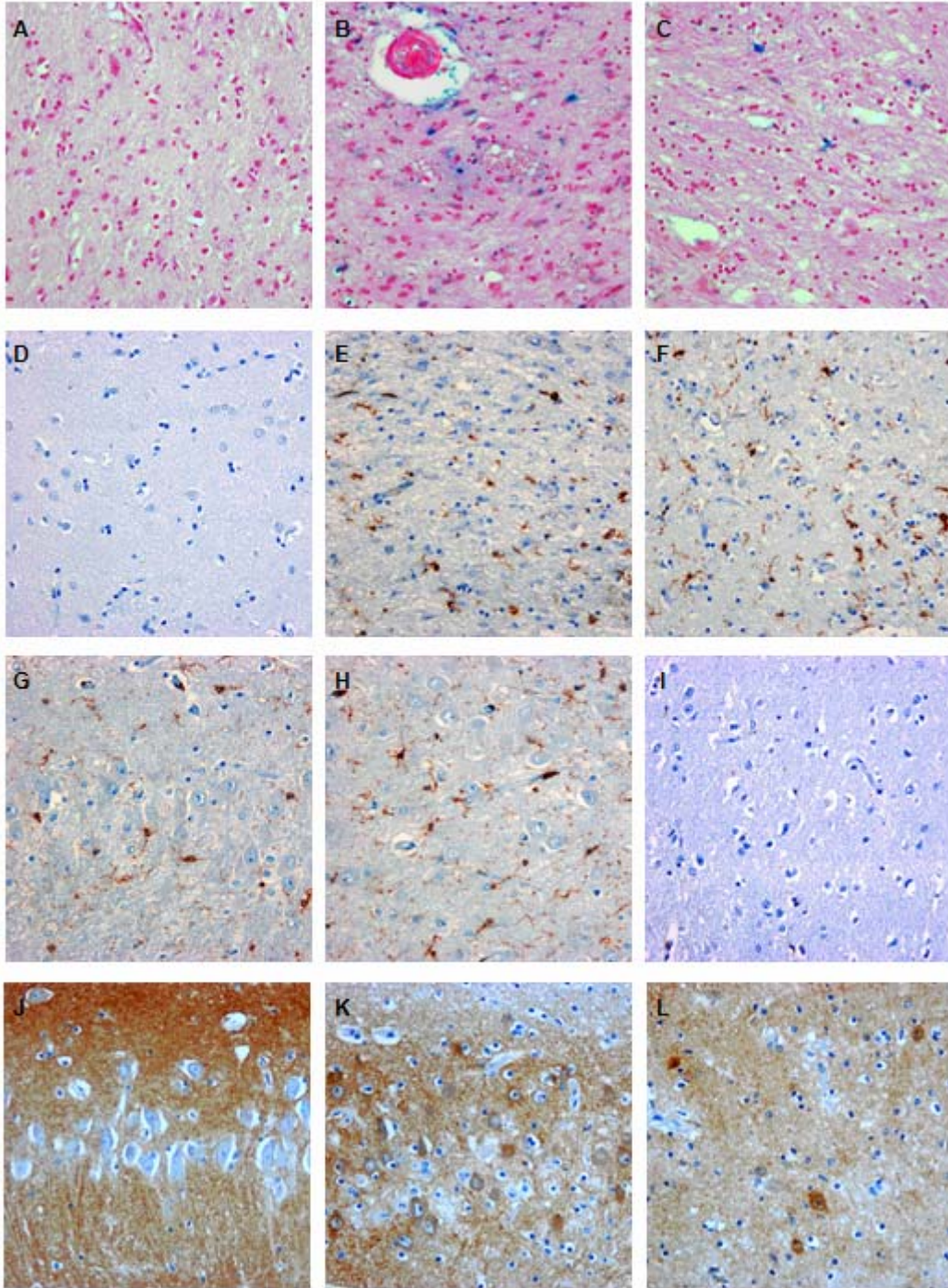


Figure 5 Specific accumulations in striatum and hippocampus. For Perl's Prussian blue stains, iron depositions were not found in nucleus accumbens (A, ChAc 3), but were found in caudate nucleus (B, ChAc 3) and internal globus

pallidus (C, ChAc 5). For Cr3/43 stain, the caudate nucleus of NC 1 was not immunoreactive (D). Meanwhile, strong immunoreactivity was observed in the caudate nucleus (E) and putamen (F) of ChAc 3, and cornu ammonis 2/3 (G) and CA4 (H) of ChAc 7, but not in the nucleus accumbens (I, ChAc 3). For α -synuclein stain, no positive-stained neurons were found in the cornu ammonis 2/3 of NC 1 (J). In contrast, positive-stained neurons were found in the cornu ammonis 2/3 of ChAc 2 (K) and caudate nucleus of ChAc 8 (L). Scale bars: 10 μ m.

4.4 Stereology of ChAc brain

The results of volume, total cell number and cell density in the striatum are listed in Table 4 and Figure 6. The mean volume of the striatum was $2.32 \pm 0.81 \text{ cm}^3$ in the 3 ChAc cases, which is practically identical with HD cases (Mann-Whitney U test, $P = 0.786$) and 53% lower than normal controls (Mann-Whitney U test, $P = 0.036$). The mean total number of small striatal neurons in the ChAc cases was $3.36 \times 10^6 \pm 2.44 \times 10^6$, which was reduced by 65% compared with HD cases (Mann-Whitney U test, $P = 0.071$) and reduced by 96% compared with normal controls (Mann-Whitney U test, $P = 0.036$). Concerning the density of small striatal neurons, it was the lowest in ChAc cases $1.29 \times 10^6 \pm 706 \times 10^3$ per cm^3 , with 70% decrease compared with HD cases (Mann-Whitney U test, $P = 0.036$) and 92% decrease compared with normal controls (Mann-Whitney U test, $P = 0.036$). The total number and density of glial and undefined cells in ChAc cases was $570 \times 10^6 \pm 255 \times 10^6$ and $244 \times 10^6 \pm 49 \times 10^6$ per cm^3 , which was respectively 1.1 times and 3.4 times higher than that of control cases (Mann-Whitney U test, $P = 0.036$ and $P = 0.036$). Compared with HD cases, it was higher by 1.9 times and by 1.8 times in ChAc (Mann-Whitney U test, $P = 0.036$ and $P = 0.036$). The glial index is defined as the ratio of total number of glial and undefined cells and total number of small neurons. The glial index of the ChAc cases was 73 times higher compared with controls (Mann-Whitney U test, $P = 0.036$) and still 10 higher compared with the HD cases (Mann-Whitney U test, $P = 0.036$).

Table 4 Summary of volume, total cell number and cell density in the striatum of ChAc cases

| Case no. | ChAc 1 | ChAc 8 | ChAc 9 | ChAc Mean (SD) (N = 3) | Huntington disease* Mean (SD) (N = 5) | Normal controls* Mean (SD) (N = 5) |
|--|-------------|-------------|-------------|---------------------------|--|---------------------------------------|
| Volume of striatum (cm ³) | 2.70 | 1.39 | 2.88 | 2.32 (0.81) | 2.29 (0.42) | 4.94 (0.35) |
| Total number of small striatal neurons | 3,747,006 | 744,401 | 5,577,525 | 3,356,310 (2,440,134) | 9,719,471 (3,640,895) | 82,091,442 (15,777,727) |
| Total number of glial & undefined cells | 526,903,782 | 338,288,375 | 843,357,392 | 569,516,516 (255,216,696) | 193,352,678 (26,129,142) | 272,673,990 (52,697,805) |
| Density of small striatal neurons (/cm ³) | 1,387,780 | 535,540 | 1,936,641 | 1,286,654 (706,003) | 4,277,930 (1,595,130) | 16,540,842 (2,723,271) |
| Density of glial cells & undefined cells (/cm ³) | 195,149,549 | 243,372,931 | 292,832,428 | 243,784,969 (48,842,743) | 85,648,379 (10,456,044) | 55,163,378 (9,943,716) |
| Glial index: glial cells/ small striatal neurons | 140.62 | 454.44 | 151.21 | 248.76 (178.21) | 22.59 (9.20) | 3.35 (0.53) |

ChAc= chorea-acanthocytosis; SD= standard deviation; * data of Heinsen et al. 1994

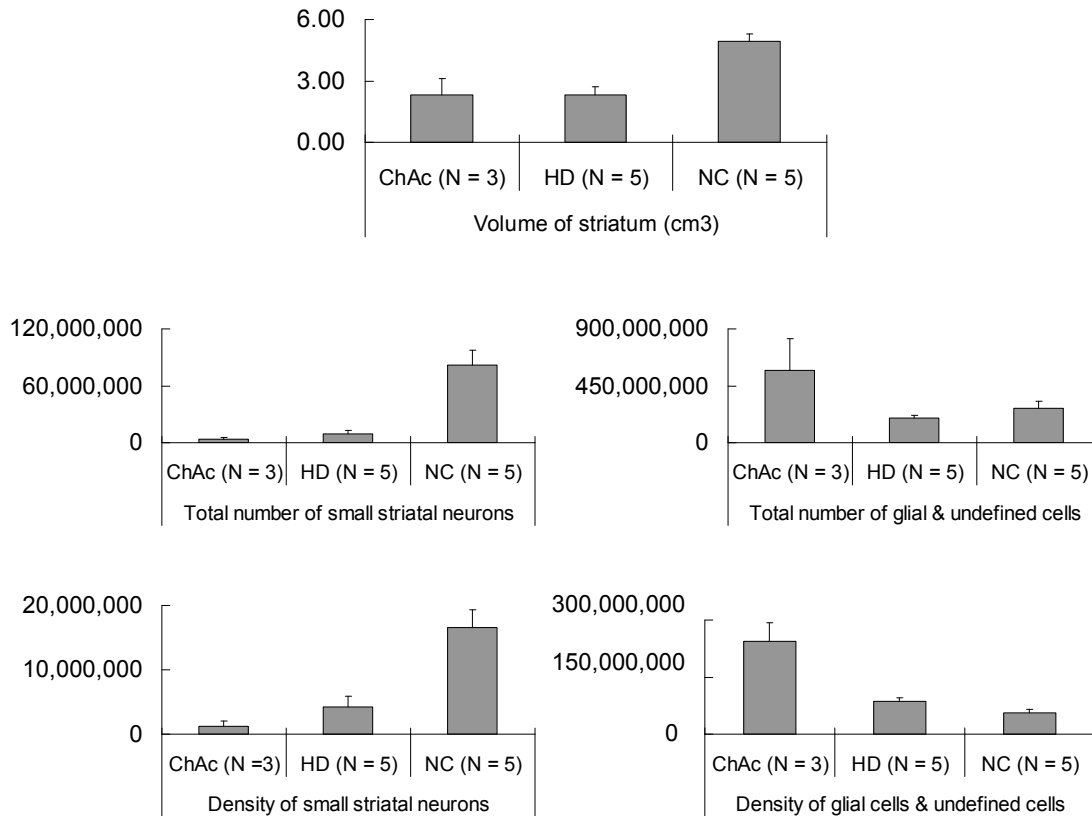


Figure 6 Volume, total cell number and cell density in the striatum of ChAc, HD and NC. No significant differences were found in the total number of small striatal neurons and volume of the striatum between ChAc and HD groups.

The results of volume, total cell number and cell density in the CPC are listed in Table 5 and Figure 7. The mean volume of the CPC was $146.2 \pm 25.7 \text{ cm}^3$ in the 3 ChAc cases, which is 19% more than HD cases (Mann-Whitney U test, $P = 0.381$) and 11% lower than normal controls (Mann-Whitney U test, $P = 0.381$). The mean total number of neurons in the CPC of ChAc cases was $669 \times 10^3 \pm 172 \times 10^3$, with 1.3 times more than that of HD cases (Mann-Whitney U test, $P = 0.024$) and 3% more than that of normal controls (Mann-Whitney U test, $P = 0.905$). The density of neurons was $4.54 \times 10^3 \pm 589$ per mm^3 in ChAc cases, with 84% more than that of HD cases (Mann-Whitney U test, $P = 0.024$) and 15% more than that of normal controls (Mann-Whitney U test, $P = 0.262$). The total number of glial cells in the CPC of ChAc cases was $29.0 \times 10^6 \pm 1.27 \times 10^6$, with 3.2 times more than that of HD cases

(Mann-Whitney U test, $P = 0.024$) and 2.0 times more than that of normal controls (Mann-Whitney U test, $P = 0.024$). The density of glial cells in the CPC of ChAc cases was $202 \times 10^3 \pm 28 \times 10^3$ per mm^3 , which was 2.5 times more than that of HD cases (Mann-Whitney U test, $P = 0.024$) and 2.5 times more than that of normal controls (Mann-Whitney U test, $P = 0.024$). The glial index in the CPC was defined as the ratio of total number of glial cells and total number of neurons. It was 2 times higher in ChAc cases compared with controls (Mann-Whitney U test, $P = 0.024$) and 86% higher compared with the HD cases (Mann-Whitney U test, $P = 0.095$).

Table 5 Summary of volume, total cell number and cell density in the centromedian-parafascicular complex of ChAc cases

| Case no. | ChAc 1 | ChAc 8 | ChAc 9 | ChAc Mean (SD) (N = 3) | Huntington disease* Mean (SD) (N = 6) | Normal controls* Mean (SD) (N = 6) |
|--|------------|------------|------------|------------------------|--|---------------------------------------|
| Volume of CPC (mm ³) | 171.6 | 120.3 | 146.6 | 146.2 (25.7) | 122.4 (33.4) | 164.4 (26.0) |
| Total number of neurons | 788,637 | 472,036 | 747,186 | 669,286 (172,076) | 291,763 (60,122) | 646,952 (129,668) |
| Total number of glial cells | 30,344,809 | 27,837,724 | 28,784,381 | 28,988,971 (1,266,002) | 6,961,989 (2,241,543) | 9,544,191 (3,028,944) |
| Density of neurons (/mm ³) | 4,596 | 3,924 | 5,097 | 4,539 (589) | 2,473 (496) | 3,951 (559) |
| Density of glial cells (/mm ³) | 176,835 | 231,403 | 196,346 | 201,528 (27,651) | 56,879 (22,927) | 58,054 (11,321) |
| Glial index: glial cells/neurons | 38.5 | 59.0 | 38.5 | 45.3 (11.8) | 24.4 (8.1) | 15.0 (5.2) |

ChAc= chorea-acanthocytosis; CPC = centromedian-parafascicular complex; SD= standard deviation; * data of Heinsen et al. 1996

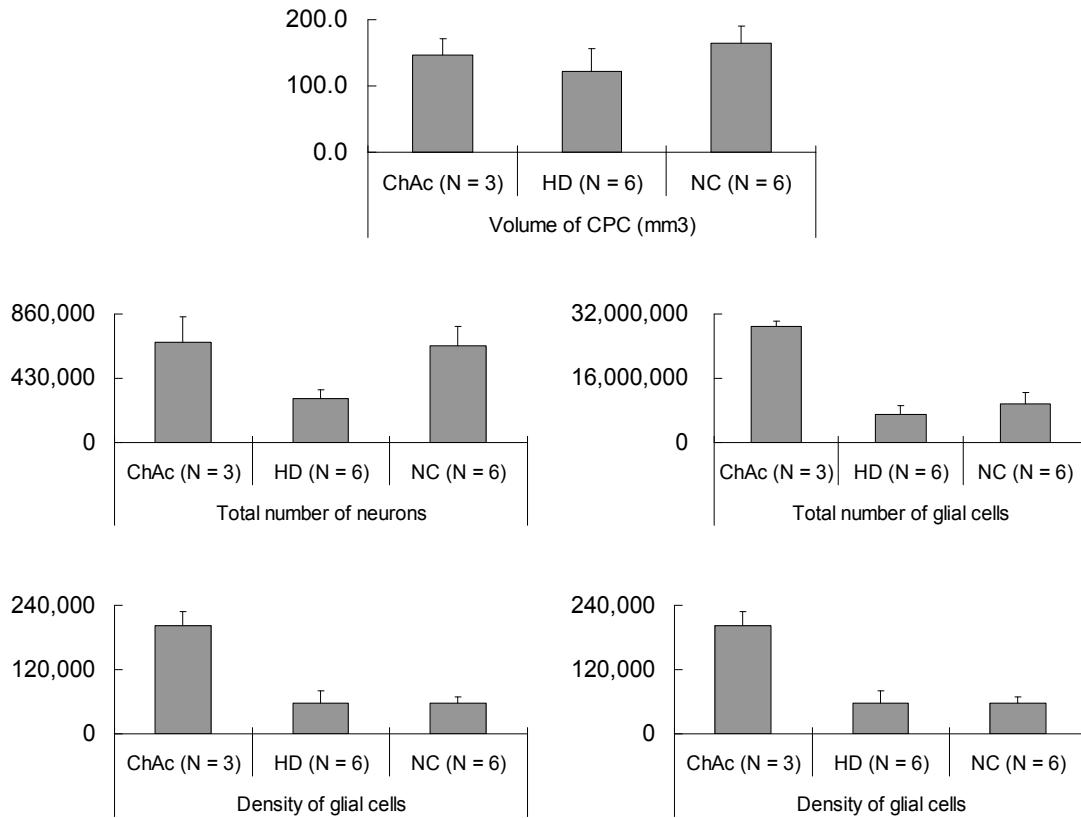


Figure 7 Volume, total cell number and cell density in the CPC of ChAc, HD and NC. Significant differences were found in the total number and density of glial cells between ChAc and NC groups, and in the total number and density of neurons and total number and density of glial cells between ChAc and HD groups.

The results of volume, total cell number and cell density in the cerebral cortex are listed in Table 8 and Figure 8. The mean volume of the cerebral cortex was 126 ± 16 cm³ in the 3 ChAc cases, which is 17% more than that of HD cases (Mann-Whitney U test, $P = 0.143$) and 9% lower than that of normal controls (Mann-Whitney U test, $P = 0.393$). The mean total number of neurons in the cerebral cortex of ChAc cases was $3.21 \times 10^9 \pm 1.10 \times 10^9$, which was reduced by 19% compared with HD cases (Mann-Whitney U test, $P = 0.571$), and reduced by 46% compared with normal controls (Mann-Whitney U test, $P = 0.036$). Concerning the density of neurons, it was $25.2 \times 10^3 \pm 5.85 \times 10^3$ per mm³ in ChAc cases, by 32% decrease compared with HD cases (Mann-Whitney U test, $P = 0.036$) and 42% decrease compared with normal

controls (Mann-Whitney U test, $P = 0.036$). The total number of glial cells in the cerebral cortex of ChAc cases was $19.8 \times 10^9 \pm 2.16 \times 10^9$, and the density of glial cells was $175 \times 10^3 \pm 45.8 \times 10^3$ per mm^3 . The glial index in the cerebral cortex of ChAc cases was 6.79, which was defined as the ratio of total number of glial cells and total number of neurons.

Table 6 Summary of volume, total cell number and cell density in the cerebral cortex of ChAc cases

| Case no. | ChAc 1 | ChAc 8 | ChAc 9 | ChAc Mean (SD) (N = 3) | Huntington disease* Mean (SD) (N = 5) | Normal controls* Mean (SD) (N = 5) |
|--|----------------|----------------|----------------|-----------------------------------|--|---------------------------------------|
| Volume of cerebral cortex (cm ³) | 114 | 119 | 144 | 126 (16) | 108 (12) | 138 (8) |
| Total number of neurons | 2,942,344,872 | 2,270,305,456 | 4,424,152,469 | 3,212,267,599 (1,102,001,791) | 3,990,218,236 (218,282,961) | 5,974,265,656 (320,705,314) |
| Total number of glial cells | 19,357,787,159 | 22,143,796,388 | 17,889,629,682 | 19,797,071,076 (2,160,835,801) | n.a. | n.a. |
| Density of neurons (/mm ³) | 25,810 | 19,078 | 30,723 | 25,204 (5,846) | 37,147 (3,344) | 43,300 (3,187) |
| Density of glial cells (/mm ³) | 213,668 | 186,082 | 124,234 | 174,661 (45,798) | n.a. | n.a. |
| Glial index: glial cells/neurons | 6.58 | 9.75 | 4.04 | 6.79 (2.86) | n.a. | n.a. |

ChAc= chorea-acanthocytosis; n.a.= not available; SD= standard deviation; * data of Heinsen et al. 1994

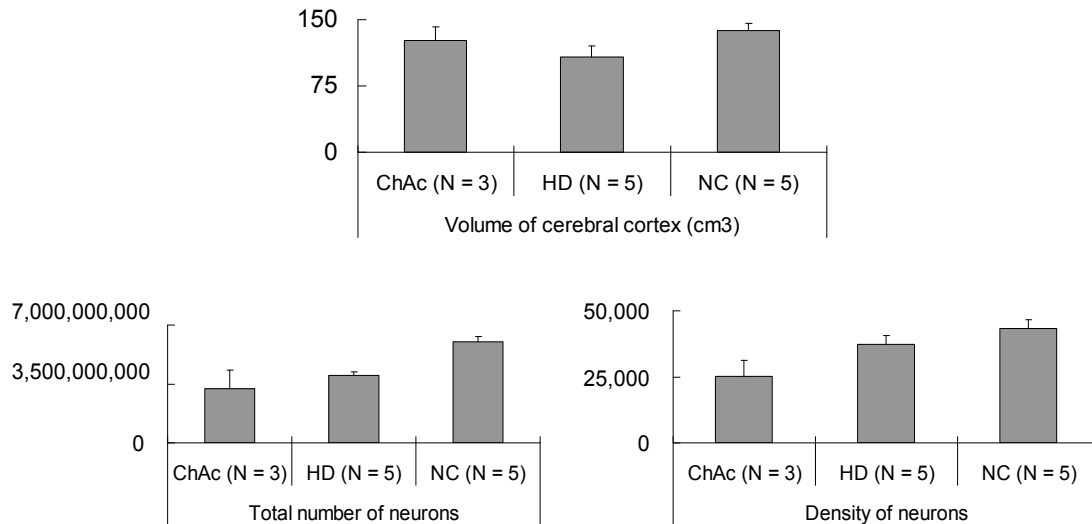


Figure 8 Volume, total cell number and cell density in the cerebral cortex of ChAc, HD and NC. Significant differences were found in the total number and density of neurons between ChAc and NC groups, and in the density of neurons between ChAc and HD groups.

4.5 Normal distribution of Chorein in the brain and peripheral organs

Western blot of different brain regions (Figure 9) showed that full length chorein was present in all examined brain regions of normal controls. No chorein expression was found in CSF.

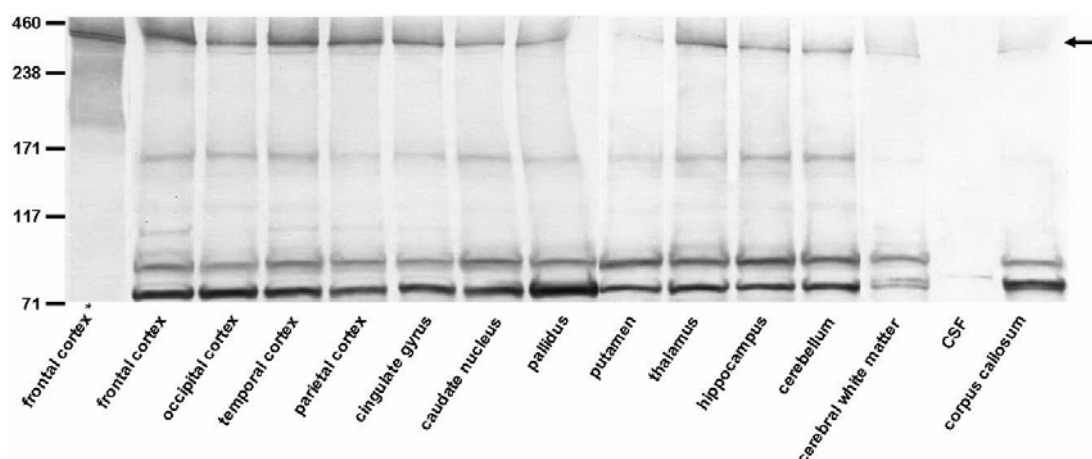


Figure 9 Chorein levels in different brain regions of a normal proband. Marker levels are given in kDa, the arrow marks full length chorein. Asterisk (*) lane was developed with antibody HPA021662 (concentration 1:1000), which was also used for immunohistochemistry. All other lanes were developed with antibody anti-chor1.

In immunohistochemistry (Figure 10) of the striatum, chorein immunoreactivity was found in the caudate nucleus, putamen, GPi and GPe. Medium and large striatal neurons were labeled diffusely in the perinuclear cytoplasm, as well as in the neuropil, but not in the nucleus. Immunohistochemistry of other non-brain organs showed chorein immunoreactivity located in the seminiferous tubule, myocardial fibres, splenic corpuscle and intestinal glands (Figure 10). Furthermore, only minor reactivity could be seen in renal cortex and proximal tubules and lung.

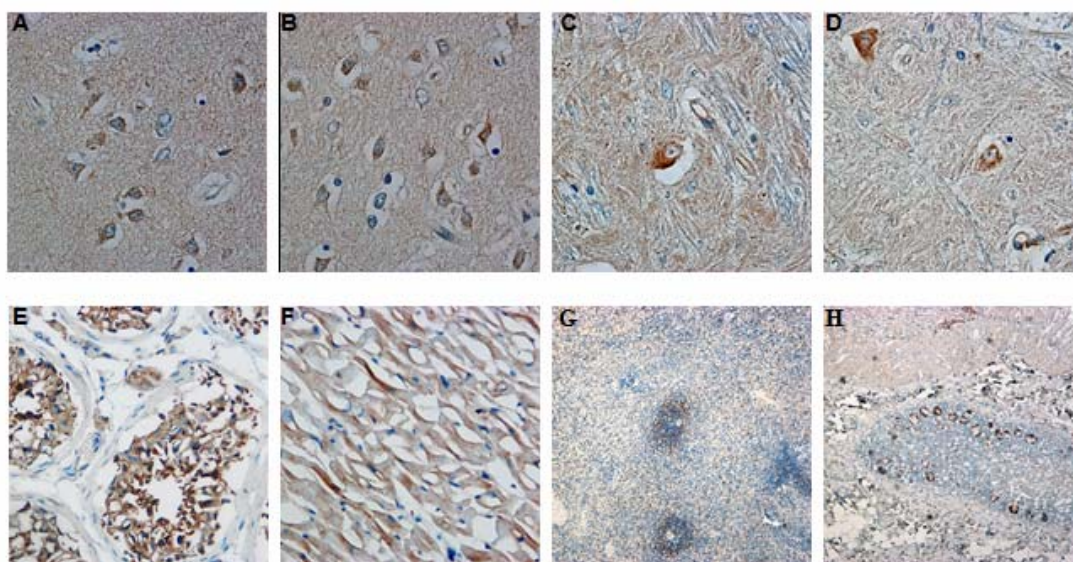


Figure 10 Chorein immunohistochemistry with antibody HPA021662 (concentration 1:50). Chorein immunoreactivity was found in the caudate nucleus (A), putamen (B), GPi (C) and GPe (D). Medium and large striatal neurons were labeled diffusely in the perinuclear cytoplasm, as well as in the neuropil, but not in the nucleus. Immunohistochemistry of other non-brain organs showed chorein immunoreactivity located in the seminiferous tubule (E), myocardial fibres (F), splenic corpuscle (G) and intestinal glands (H). Scale bars: 50µm in A-D, 100µm in E and F, and 500µm in G and H.

Normalized to standard protein concentration of brain tissue homogenate (1mg/ml), the quantitative analysis of chorein immunoblot (Figure 11) illustrated that chorein was

strongly present in testis (10.43x) and still at fair levels in heart (1.16x), bone marrow (1.03x) and muscle (0.9x). However, in pancreas (0.33x), stomach (0.32x), intestine (0.26x) and colon (0.34x) chorein levels were reduced compared to brain. In addition, chorein was also distributed in the spleen (0.68x), liver (0.58x), lung (0.57x), kidney (0.54x), ovary (0.53x) and peripheral nerve (0.51x).

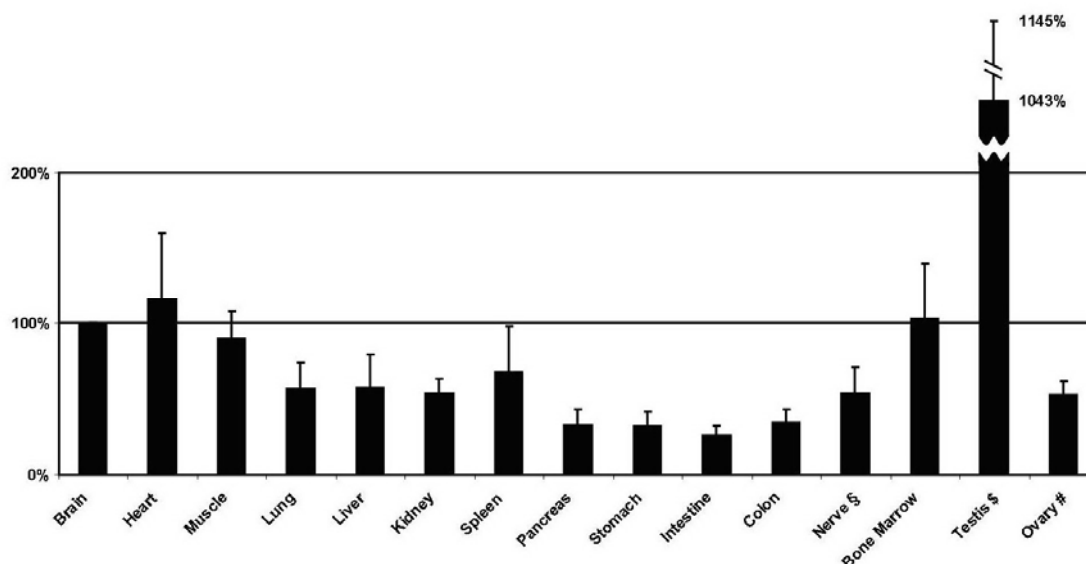


Figure 11 Qualitative chorein in different organs of normal controls. The suspected chorein band was found in all organs and normalized to standard brain content of chorein. We examined 6 samples of nerve tissue (\$), 4 samples of testis tissue (\$), 3 samples of ovary tissue (#) and 7 samples of all other non-brain organs.

4.6 ChAc pathology in muscle

H&E and MHC stained sections showed a moderate neurogenic process (Figure 12, A-E). Nevertheless, scattered neurogenic angulated atrophic fibres were seen. All muscle samples displayed signs of neurogenic changes with fibre group atrophies, fibre type grouping and predominance, and angulated fibres. In two muscles, obvious fibre group atrophies as well as angulated fibres were seen (cases 7 and 9). Atrophic fibres belonged to both fibre types in case 9, while case 7 showed predominant atrophy of type 2 fibres. Using immunohistochemistry, chorein was found to be distributed along the sarcoplasm and myofibril in normal control (Figure 12, F).

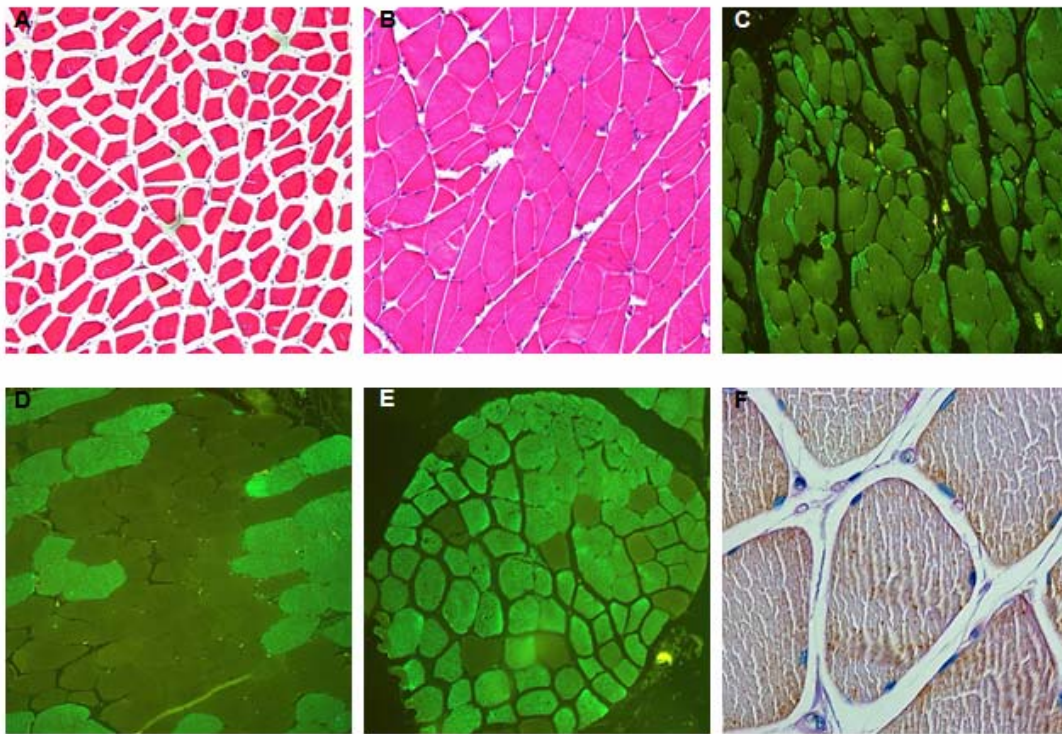


Figure 12 Muscle histology. (A) Autopsy muscle of case 9 demonstrates numerous atrophic and angulated fibres. (B, C) Autopsy muscle of case 7 shows most impressive fibre size variation, angulated fibres, and a predominance of type 1 fibres (dark green) with obvious atrophy of type 2 fibres (bright green). (D) Case 6 biopsy shows classic fibre-type grouping of type 1 (dark green) and type 2 (bright green). (E) Case 4 biopsy shows a majority of type 2 fibres (bright green). Chorein (brown) is distributed along the sarcoplasm and myofibril in normal control (F). Stainings: A, B H&E; C-E myosin heavy chain fast isotype; F anti-VPS13A immunohistology (brown), restrained with PAS. Scale bars: 200µm in A and B, 100µm in C-E, and 50 µm in F.

Six muscles in our series (cases 1, 3, 5, 8, 9, 10) showed an equal representation of both fibre types. Three samples showed predominance of type 2 fibres (cases 2, 4 and 6), and type 1 fibres (cases 7), respectively (Table7). Three muscles showed increased fibre size variation (cases 1, 7, 8), and pronounced endomysial fibrosis was present in one muscle (case 8). In addition to this, a slight increase in the number of internalized nuclei was notable (< 5% = normal; 6-14 % = increased; > 15% = clearly

pathological). There was no evidence for necrosis (HE), or other structural alterations, like nemaline rods, or accumulation of glycogen (PAS).

Table 7 Muscle histology

| Case no. | Muscle | Myopathic alterations | | | | Neurogenic alterations | | | |
|----------|-------------------|--------------------------------|----------|-------------------------|---------------------|------------------------|------------------|---------------------|-------------------------|
| | | Increased fibre size variation | Necrosis | Internalized nuclei [%] | Endomyrial fibrosis | Fibre group atrophies | Angulated fibres | Fibre-type grouping | Fibre-type predominance |
| 1 | Biceps (B) | (+) | - | 14 | - | - | (+) | ++ | - |
| 2 | Biceps (B) | - | - | 5 | - | - | (+) | - | 2:++ |
| 3 | Biceps (B) | - | - | 11 | - | - | - | ++ | - |
| 4 | Biceps (B) | - | - | 9 | (+) | - | - | ++ | 2:++ |
| 5 | Biceps (B) | - | - | 4 | - | (+) | (+) | + | - |
| 6 | Biceps (B) | - | - | 4 | - | - | - | - | 2:++ |
| 7 | Deltoides (A) | + | - | 12 | - | - | + | - | 1:++ |
| 8 | Gastrocnemius (B) | ++ | - | 17 | ++ | - | (+) | ++ | - |
| 9 | Psoas (A) | - | - | 8 | - | - | + | - | - |
| 10 | Quadriceps (B) | - | - | 10 | - | - | - | + | - |

A=autopsy, B=biopsy; - indicates absent; (+) indicates subtle/rare; + indicates moderate/occasional; ++ indicates pronounced/frequent. The baseline information is provided in Table 1.

The results of the morphometric analysis demonstrated a decrease of mean fibre diameters in three muscles (cases 4, 7, 9), increased variability coefficients of both fibre types' diameters in three muscles (cases 1, 7, 8), pathological atrophy coefficients in seven muscles (cases 1-5, 7, 9), and pathological hypertrophy coefficient of type 1 fibres in one muscle (case 8) (Table 8 and Figure 13). The mean values of fibre diameter, variability coefficient and hypertrophy coefficient in type 1 and 2 fibres were in the normal range, but the mean values of atrophy coefficient were abnormal in type 1 and 2 fibres. By Mann-Whitney U test, there was no significant difference between type 1 and 2 fibres in fibre diameter, variability coefficient, atrophy coefficient and hypertrophy coefficient.

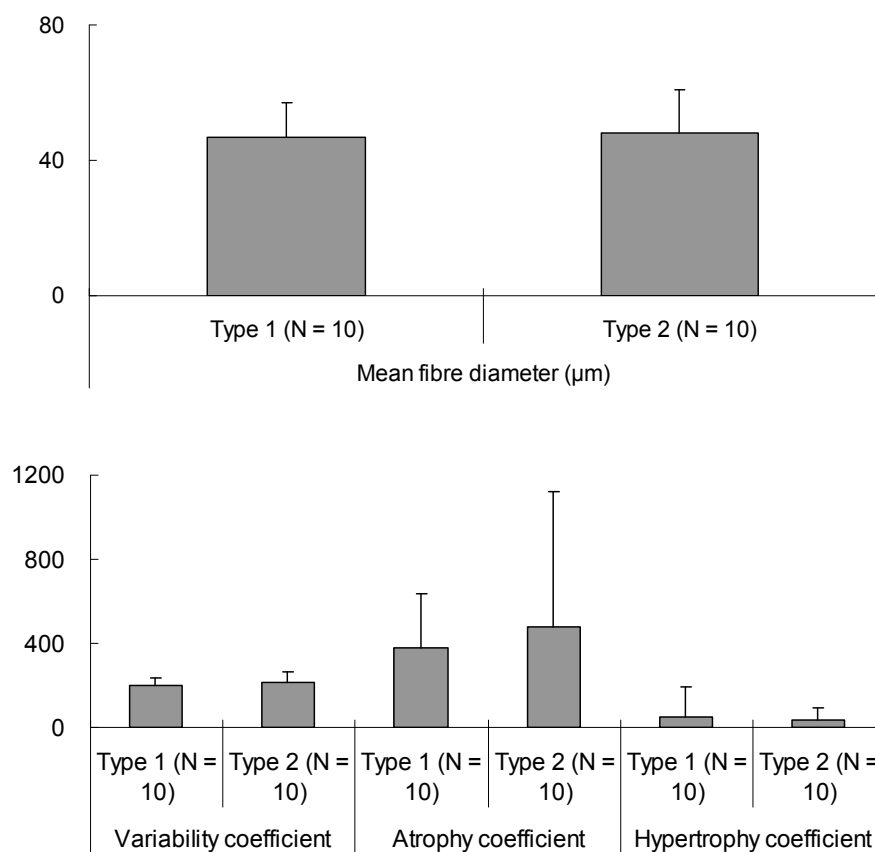


Figure 13 Morphometry. There was no significant difference between type 1 and 2 fibres in fibre diameter, variability coefficient, atrophy coefficient and hypertrophy coefficient.

Table 8 Morphometry

| Case no. | Mean fibre diameter (μm) | | Variability coefficient | | Atrophy coefficient | | Hypertrophy coefficient | |
|----------|---------------------------------------|-----------|-------------------------|------------|---------------------|-------------|-------------------------|--------|
| | Type 1 | Type 2 | Type 1 | Type 2 | Type 1 | Type 2 | Type 1 | Type 2 |
| 1 | 47 | 46 | 214 | 272 | 210 | 400 | 0 | 0 |
| 2 | 41 | 50 | 211 | 207 | 560 | 170 | 0 | 10 |
| 3 | 40 | 48 | 204 | 227 | 540 | 240 | 0 | 0 |
| 4 | 39 | 37 | 198 | 221 | 670 | 780 | 0 | 0 |
| 5 | 42 | 47 | 151 | 165 | 420 | 170 | 0 | 0 |
| 6 | 53 | 61 | 197 | 177 | 110 | 40 | 20 | 40 |
| 7 | 40 | 24 | 203 | 281 | 600 | 2130 | 0 | 0 |
| 8 | 69 | 61 | 276 | 267 | 20 | 110 | 450 | 140 |
| 9 | 39 | 37 | 136 | 143 | 620 | 750 | 0 | 0 |
| 10 | 60 | 67 | 192 | 182 | 70 | 0 | 30 | 150 |

Mean fibre diameter (norm. 40-80 μm), variability (norm. < 250), atrophy (norm. < 350) and hypertrophy (norm. < 350) coefficients were calculated for type 1 and type 2 fibres, respectively. Pathological values are marked in bold.

4.7 ChAc pathology in nerve

Cross sections of sural nerves of cases 8 and 9 (Figure 14) showed no overt abnormalities in H&E and GT staining. There was no significant loss of myelinated fibres in MBP staining, loss of neurofilament protein in neurofilament staining, and endoneural or perineural fibrosis in EvG staining.

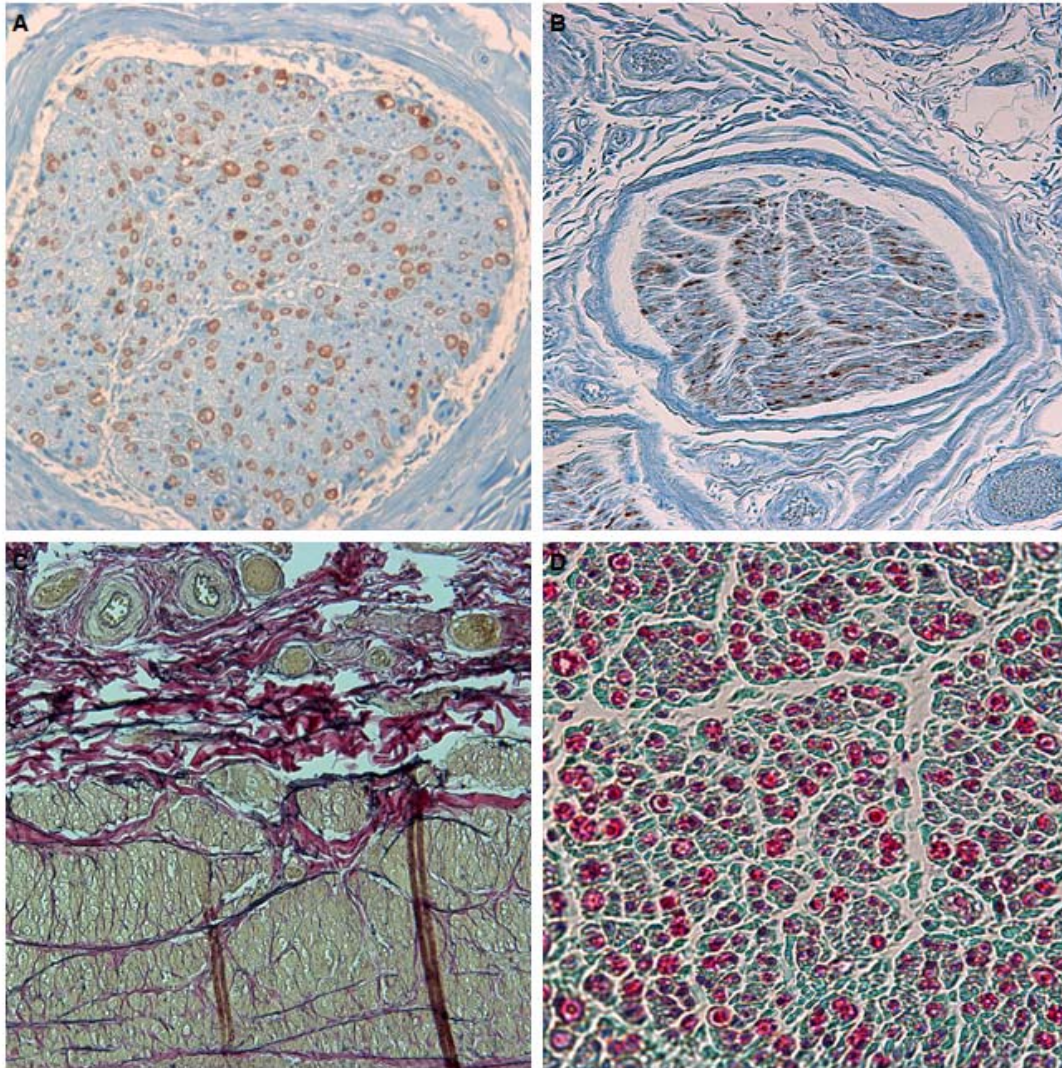


Figure 14 Nerve histology. The paraffin slides of sural nerves of cases 8 and 9 demonstrate no overt abnormalities in MBP (A, case 9), Neurofilament (B, case 9), EvG staining (C case 9) and GT (D case 8). Scale bars: 100 μ m in A, 200 in B and C, and 50 μ m in D.

4.8 Epidemiology of NA in China

We found a total of 36 studies with 53 cases (27 male and 26 female) (Table 9). All these patients were clinically diagnosed as either NA or ChAc. No cases were confirmed by gene test or chorein Western blot. No report of MLS was identified. The cases originated from 15 Chinese provinces, with 12 cases from Beijing, 7 cases from Anhui and 5 cases from Heilongjiang.

Table 9 Baseline information of NA cases from China

| Place of diagnosis | Year of publication | Ref. | Case number | Gender | AOO | Initial symptoms | Reported diagnosis |
|--------------------|---------------------|--|-------------|--------|-------|---------------------------------|--------------------|
| Anhui | 1984 | (Yang et al. 1984) | 2 | 2M, 0F | 19;27 | Orof. (n=1); MD & Orof. (n=1) | ChAc |
| Anhui | 1987 | (Yang et al. 1987) | 2 | 2M, 0F | 26;32 | DYA (n=1); MD & Orof. (n=1) | ChAc |
| Anhui | 2000 | (Sun 2000) | 2 | 0M, 2F | 45;46 | MD (n=1); PSY (n=1) | ChAc |
| Anhui | 2004 | (Yang et al. 2004) | 1 | 1M, 0F | 39 | Orof. & MD | ChAc |
| Beijing | 2005 | (Bo et al. 2005) | 1 | 0M, 1F | n.a | MD | ChAc |
| Beijing | 2005; 2012 | (Zhou et al. 2012; Liu et al. 2005; Wei et al. 2005) | 8 | 2M, 6F | 10-35 | Orof. (n=4); MD (n=3); PN (n=1) | NA |
| Beijing | 2007 | (Zhou et al. 2007) | 2 | 2M, 0F | 27;37 | MD (n=1); EPI (n=1) | ChAc |
| Beijing | 2010 | (Hu et al. 2010) | 1 | 1M, 0F | 11 | n.a. | NA |
| Gansu | 2009 | (Tang 2012) | 1 | 1M, 0F | 20 | MD | NA |
| Guangdong | 2003 | (Zhang et al. 2003) | 1 | 1M, 0F | 42 | Orof. | ChAc |
| Heilongjiang | 1989 | (Zheng et al. 1989) | 1 | 0M, 1F | 36 | DYA & Orof. | ChAc |
| Heilongjiang | 1989 | (Zhang et al. 1989) | 2 | 1M, 1F | 9,11 | Orof. (n=2) | ChAc |
| Heilongjiang | 1990 | (Yang and Liang 1990) | 1 | 0M,1F | 38 | Orof. | ChAc |
| Heilongjiang | 2003 | (Qu et al. 2003) | 1 | 0M, 1F | 35 | Orof. | ChAc |
| He'nan | 2005 | (Wang and Cao 2005) | 1 | 0M, 1F | 30 | Orof. & EPI | NA |
| He'nan | 2011 | (Zhang and Zhao 2011) | 2 | 1M, 1F | 30;31 | MD (n=1); Orof. (n=1) | ChAc |
| He'nan | 2012 | (Ma et al. 2012) | 1 | 1M, 0F | 43 | MD | ChAc |
| Hubei | 2007 | (Zhao and Mao 2007) | 1 | 0M, 1F | 28 | Orof. | NA |
| Jiangsu | 2012 | (Zhao et al. 2012) | 1 | 0M, 1F | 20 | MD & Orof. | ChAc |
| Liaoning | 1989 | (Dong et al. 1989) | 1 | 1M, 0F | 28 | Orof. | ChAc |
| Neimenggu | 2005 | (Luo and Zhao 2005) | 1 | 1M, 0F | 32 | EPI | ChAc |
| Neimenggu | 2007 | (Sa ru la et al. 2007) | 1 | 1M, 0F | 34 | MD | ChAc |
| Neimenggu | 2012 | (Jia et al. 2012) | 1 | 1M, 0F | 38 | Orof. | ChAc |
| Qinghai | 2006 | (Zeng 2006) | 1 | 0M, 1F | 24 | MD | NA |
| Shandong | 2001 | (Liu et al. 2001) | 3 | 0M, 3F | 20-21 | MD (n=3) | NA |
| Shanghai | 2008 | (Chen et al. 2008) | 1 | 0M, 1F | 33 | MD & Orof. | ChAc |
| Shanghai | 2008 | (Jiang and Zhou 2008) | 1 | 1M, 0F | 5 | DYT | NA |
| Shanghai | 2010 | (Jiang 2010) | 1 | 0M, 1F | 55 | Walking instability | NA |
| Shanghai | 2012 | (Zhang et al. 2012) | 3 | 2M, 1F | 31-74 | MD (n=1); GD (n=2) | NA |
| Shanxi | 2004 | (Cui et al. 2004; Cui et al. 2005) | 3 | 2M, 1F | 26-30 | EPI (n=2); Orof. (n=1) | ChAc |
| Sichuan | 2012 | (Li et al. 2012) | 2 | 2M, 0F | 17;18 | Orof. (n=2) | ChAc |
| Sichuan | 1988 | (He and Zhang 1988) | 1 | 1M, 0F | 25 | Orof. | ChAc |
| Taiwan | 2006 | (Lin et al. 2006) | 1 | 0M, 1F | 31 | MD | NA |

AOO=age of onset; ChAc=chorea-acanthocytosis; DYT=dystonia; DYA=dysarthria; EPI=epilepsy; F=female; GD=gait disturbance; M=male; MD= movement disorders (chorea or involuntary movements); NA= neuroacanthocytosis; n.a.=not available; No.=number; Orof.=orofacial dyskinesias; PN=parkinsonism; PSY=psychiatric symptoms; Ref.=reference

The age of onset was from 5 to 74 years, most of them (N = 46, 87%) before 40 years. The common initial symptoms were orofacial dyskinesias (N = 19, 36%) and movement disorders in limbs or trunk (N = 18, 34%). Dysarthria, epilepsy, gait disturbance, parkinsonism and psychiatric symptoms can be also presented as early symptoms. An elevated proportion of acanthocytes on blood films was regarded as the key indicator. Diagnosis was mainly based on hyperkinetic movement disorders and elevated acanthocytes in the blood with exclusion of other possible diseases.

In Figure 15, we summarized the clinical and laboratory findings in Chinese published NA cases. The most frequent findings were involuntary movements (N = 48, 91%). Orofacial dyskinesias were found in 42 patients (79%). In addition, dystonia (N = 40, 75%), dysarthria (N = 35, 66%), caudate atrophy or enlarged lateral ventricles on neuroimaging (N = 32, 60%) and elevated creatine kinase (N = 27, 51%) were also common in NA cases. There were 10 patients (19%) suffered from epilepsy and 14 patients (26%) with psychiatric symptoms.

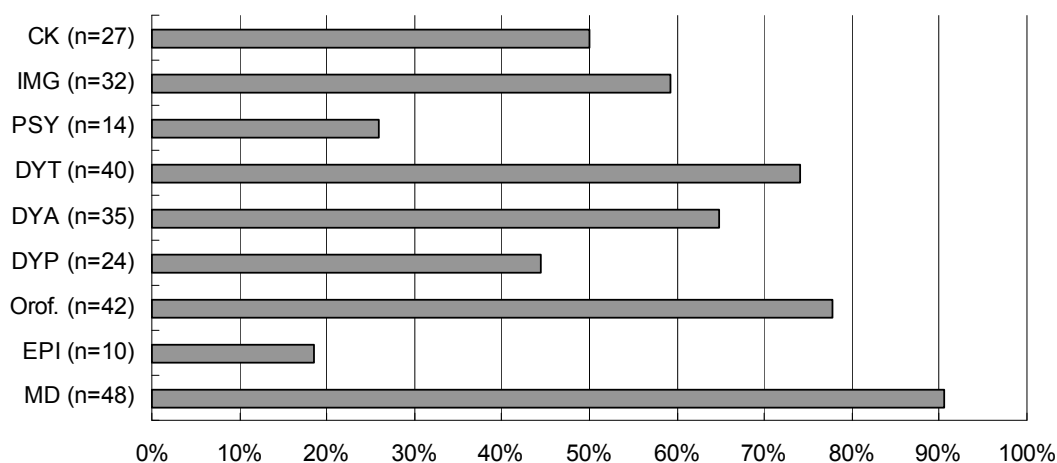


Figure 15 Clinical and laboratory positive findings in Chinese patients diagnosed as neuroacanthocytosis (N=53). CK= Creatine kinase elevated; IMG= Caudate atrophy or enlarged lateral ventricles on neuroimaging; PSY= Psychiatric symptoms; DYT= Dystonia; DIA= Dysarthria; DYP= Dysphagia; Orof.= Orofacial dyskinesias; EPI= Epilepsy; MD= hyperkinetic movement disorders (chorea or involuntary movements).

5 Discussion

5.1 ChAc pathology in striatum

Significant decreases of SP and ENK are found in ChAc, compared to the normal control (Figure 2 and 3), which suggests that impairments of ENK and SP projecting systems are involved in ChAc. There are two projection systems in the basal ganglia, that is, direct and indirect pathways. In indirect pathway ENK containing striatal neurons project to the Gpe and subthalamic nucleus, while in direct pathway SP containing striatal neurons project to Gpi and substantia nigra. The indirect pathway has the GABAergic inhibition to the direct pathway via influencing the Gpi and substantia nigra. Once this inhibition decreases, the hyperkinetic such as chorea could be seen. In ChAc, both the direct and indirect pathways are found to be affected, which can explain the early presentation of parkinsonism in certain ChAc patients (Bostantjopoulou et al. 2000; Peppard et al. 1990).

The previous investigations reported a decreased GAD activity in HD by biochemical assays (Storey and Beal 1993). In immunohistochemistry, striatal projection neurons were usually not GAD stained, which is due to the rapid transportation of GAD from the soma to processes and terminal buttons (Rice et al. 2011). GAD is mainly distributed in the matrix of caudate nucleus and putamen. In comparison with normal control, decreased GAD architecture is found in dorsal striatum of ChAc (Figure 1). The GAD-positive cell bodies can be seen in all pallidal structures such as the globus pallidus and substantia nigra (Beckstead and Kersey 1985). We found reduced GAD-positive areas in the globus pallidus of ChAc and HD compared to normal control, but statistical significance was only found in GPi between ChAc and control groups (Figure 3).

CALB is generally regarded as neuroprotective in central nervous disease, e.g. stroke and Parkinson's disease (Yenari et al. 2001; Heizmann and Braun 1995). However,

the number of CALB-stained neurons was not significantly changed in the three groups (Figure 2). It has been confirmed that CALB is mainly present in the striatal projection neurons (Ferrante et al. 1991), and there were also light stains of CALB in the cells and neuropils of globus pallidus (Domaradzka-Pytel et al. 2007). The decreased CALB neurons in dorsal striatum might be the subsequent result of the impairments in the projection neurons, which is not so conspicuous as the decreased SP and ENK neurons in ChAc. Compared to normal controls, the architecture of CALB in dorsal striatum is stronger in ChAc, which suggested there is an increased CALB distribution in the matrix. The absence of chorein is the predominant change in ChAc, and influences the transport of proteins (Velayos-Baeza et al. 2008). Therefore, it is reasonable to presume that the increase of calcium-binding proteins in the matrix might be associated with the loss of chorein.

5.2 ChAc pathology in hippocampus

Based on the rich SP immunoreactivity in normal control, SP is regarded to play the major role in the function of hippocampus. In Alzheimer's disease, reduction of SP in hippocampus has been confirmed (Jimenez-Corral et al. 2006). The decreased SP expression is distributed in the neurons and axons throughout all the subfields of hippocampus, which might contribute to the cognitive decline. Our findings suggest the impairments of SP in ChAc are not limited to the striatum, but also include the hippocampus.

ENK belongs to the endogenous opioid system and modulates learning and memory, synaptic plasticity, and emotional behaviors (Bodnar and Klein 2005; Do et al. 2002; Nieto et al. 2005). Meanwhile, elevated ENK expression has been found in the DG of hippocampus, which is considered to contribute to the cognitive impairments in Alzheimer's disease (Meilandt et al. 2008). In this study, the increased ENK immunoreactivity was diffusely located in the hilus of DG and CA3 of ChAc, which can

be associated with the cognitive decline in the ChAc patients.

GAD and CALB are believed to decrease with the aging process (Stanley and Shetty 2004; de Jong et al. 1996). However, no overt changes were found in ChAc, apart from the reduced CALB stained granule cells in DG. In epilepsy patients with hippocampal sclerosis, CALB expression in the granule cells of DG is associated with granule cell dispersion and mossy fiber sprouting, but not associated with memory function (Martinian et al. 2012). Interestingly, the predominant changes in ChAc suggest that granule cell loss and dispersion might be related to epilepsy rather than ChAc itself. Moreover, the astrogliosis of hippocampus is obvious and involved in the pathophysiology, because the ratio of astrocytes/neurons is significantly increased in the hilus of DG of ChAc patients with cognitive decline.

5.3 Specific accumulations in ChAc brain

Striatal A β plaques are found to be associated with dementia in Parkinson's disease, compared to the cases without dementia (Kalaitzakis et al. 2008). In the ChAc cohort, 6 of 8 patients were accompanied by dementia, but no classic extracellular accumulation was found in any case. However, intracellular accumulations were widely distributed in the striatum and hippocampus of normal controls and ChAc patients without significant difference. Therefore, our results suggest that intracellular A β deposition is not involved in the dementia process of ChAc.

Iron deposition has been found in the striatum of patients with neurodegenerative disease, and is believed to be a marker of neurodegeneration. In AD, iron deposition is even detected in the preclinical cases, which hints the early involvement in the pathophysiology. In ChAc cases, many of the iron-positive structures are associated with glial cells in the parenchyma, which is the pattern in AD. Moreover, there are also perivascular iron accumulations and around axons of white matter in ChAc. Interestingly, the accumbens nucleus is rarely affected by iron deposition in all the

ChAc cases, compared to caudate nucleus and putamen. Therefore, we speculated that iron deposition might be more associated with movement disorders in patients with ChAc.

Cr3/43 staining is a reliable marker of activated microglia in the parenchyma of brain. It has been reported that microglia were increased in the striatum, cortex and white matter of HD brains, and activated microglia were thought to be associated with neuron degeneration and ferritin accumulation in HD (Simmons et al. 2007; Sapp et al. 2001). In our study, activated microglia were found in the striatum of certain ChAc cases, but not correlated with striatal A β deposition. In other ChAc cases, no significantly increased microglia was found. It has been found that chorein is highly expressed in the organs of mesoderm-origin and absent in ChAc. Interestingly, microglia are derived from mesoderm. But all the other glial cells, such as astrocytes and oligodendrocytes, are originated from neuroectoderm. Thus, increased microglia in ChAc might be associated with chorein absence in the pathophysiology. The factors including acute psychotic episodes, post mortem interval, neuroleptic treatment and aging should also be considered, which can affect the number of activated microglia (Steiner et al. 2006).

The negative results of p62 and AT8 stains illustrate that ChAc is distinct from other neurodegenerative diseases, because of the absence of common inclusions such as tau accumulations. Meanwhile, one ChAc case (ChAc 8) was α -synuclein positive in the neurons of caudate nucleus and CA, but without p62 accumulations. Therefore, we can not assert α -synuclein accumulations are involved in ChAc with a possibility of precursors to Lewy bodies, which can not be detected by p62 stain like typical Lewy bodies (Paine et al. 2005; Kuusisto et al. 2003).

5.4 Stereology of ChAc brain

By stereological analysis, there was a mean 96% small striatal neuron loss in ChAc

cases, and a mean 46% cortical neuron reduction, but without neuron loss in the CPC. The previous studies suggested a mean 88% small striatal neuron loss, 33% cortical neuron reduction and 55% neuron loss in the CPC of HD cases (Heinsen et al. 1994; Heinsen et al. 1996). Comparing the number of neurons in ChAc and HD, significant differences were found in the striatum and CPC, with more severe neuron loss in the striatum of ChAc and more neurons preserved in the CPC of ChAc. There was no statistical difference in the number of cortical neurons in ChAc and HD. The findings demonstrated a different pathological change in ChAc brain compared to HD brain. Compared to HD, CPC was far less affected in ChAc, in which the number of neurons was similar to that of normal controls. Actually, previous stereological study concluded that the neuron number in CPC was not significantly changed in Alzheimer's disease and Parkinson's disease (Xuereb et al. 1991), while the meaningful reduction was found in the CPC of HD (Heinsen et al. 1996).

Neuronal depletion in the striatum and cerebral cortex of ChAc is highly significant compared to normal controls. Chorea as the predominant symptom was found in all the cases of ChAc cohort. Orofacial dyskinesia, dystonia, dysarthria and dysphagia are also commonly seen in ChAc. It is worthy of note that the striatal small neuron loss in ChAc is even more severe than HD, which can explain a variety of clinical movement disorders. In addition, the neuron loss in both striatum and cerebral cortex of ChAc may cause cognitive decline, seizure and psychiatric symptoms, although the cortical neuron loss in ChAc is not more significant compared to that of HD. Subcortical dementia was believed as the main reason for dementia in HD, and diffuse cortical neuron loss is insufficient to explain (Heinsen et al. 1994; Salmon and Filoteo 2007). For seizure, a concept of subcortical epilepsy has been raised (Badawy et al. 2013), which is different from the traditional knowledge that the site of seizure origin is cerebral cortex. Subcortical structures are also involved in the epileptiform

discharges. Moreover, stereological analysis illustrated the neuron loss in the subcortical regions of psychiatric disorders like schizophrenia (Kreczmanski et al. 2007).

In clinical neuroanatomy, the CPC can be divided into centromedian (CM) and parafascicular (Pf) nuclei, and links to both striatal parts by efferents. In general, the Pf nucleus mainly links to the caudate nucleus (associative-limbic striatum), while the CM nucleus mainly links to the putamen (sensorimotor striatum) (Sadikot et al. 1992; Sadikot and Rymar 2009). Therefore, the CM and Pf nuclei are considered to be involved in parallel processing of sensorimotor and associative-limbic information in the striatum. Although the striatum is severely affected in both ChAc and HD, the CPC seems to be not obviously changed in ChAc in comparison to HD. On the other hand, the Pf nucleus can receive afferents from the frontal eye fields and superior colliculus, and project to the supplementary eye field (Huerta et al. 1986; Parent and De Bellefeuille 1983). The neuron loss is thought to be associated with abnormal saccades in HD (Heinsen et al. 1996). In the ChAc cases for stereology, saccadic eye movement disorders were only reported in case 8. Meantime, the volume of the CPC in case 8 was the lowest, which is comparable to the volume of HD cases. Moreover, the number of neurons in this case is obviously reduced in comparison to other two ChAc cases. Considering the duration of disease in case 8 is the longest, the CPC may be affected in the late stage of ChAc.

Although the differences of total volume and cell density were found in the different diseases and normal controls, they can be also influenced by the technical factors. Therefore, they are not further discussed in the dissertation. The most common feature in ChAc is dramatically increased glial cells, no matter in the striatum, cerebral cortex or CPC. On the contrary, the total number of glial cells is widespreadly decreased in HD compared with normal controls. The findings suggest that gliosis

may play a key role in the pathophysiological process of ChAc, which is quite different from HD.

5.5 Chorein distributions in human tissues

Chorein is expressed in the caudate and putamen (neostriatum) of normal controls, but absent in ChAc patients. This finding probably corresponds with the clinical picture of patients showing a choreatic movement disorder and to the imaging data showing atrophy of these areas during the course of disease. Slightly lower chorein levels are found in the globus pallidus (palaeostriatum). This might be due to the fact that the globus pallidus is traversed by numerous myelinated axons of the striato-pallidonigral bundle, which contains much white matter decreasing the number of neurons per area. This might be the reason why the globus pallidus is relatively less involved in the pathological process of ChAc.

Chorein is present in the hippocampus, amygdala, frontal cortex and striatum in normal controls, which might explain the progressive neuropsychiatric and cognitive disorder of ChAc patients who are lacking chorein protein in these areas. Neuropsychiatric symptoms and cognitive decline occur in certain ChAc patients and usually consist of obsessive-compulsive disorders, depression, anxiety and symptoms similar to frontal lobe syndromes affecting executive functions and to a lesser degree memory functions (Danek et al. 2004; Walterfang et al. 2008). Additionally, the striatum especially with its ventral parts is also involved in the loops that modulate the output to the cortex, which could cause comorbid negative influences on motor as well as cognitive and emotional abilities (Kimura and Matsumoto 1997).

On a cytological level, chorein is clearly pronounced in the perinuclear cytoplasm and to a lesser extent in the neuropil, while nuclei are spared. This finding corresponds to previous descriptions of subcellular chorein localization (Kurano et al. 2007). Chorein

is believed to regulate the transport of proteins between the trans-Golgi network and the prevacuolar compartment (Brickner and Fuller 1997; Velayos-Baeza et al. 2004; Velayos-Baeza et al. 2008). The involvement of chorein in cyto-skeleton architecture and ion channels of erythrocyte-membranes might explain the slight presence of chorein in the white matter dominant areas (Bosman et al. 1994; De et al. 2004). However, the pathophysiological process in general and the connection between erythrocyte pathology and brain tissue in particular is still unknown.

In different body organs, chorein was highly present in testis, heart, bone marrow, brain and muscle. Besides brain this comprises many organs developing from the mesoderm. In contrast, lower levels of chorein are found in the digestive organs like pancreas, stomach, intestine and colon that are deriving from the endoderm. Also considering the conservation of chorein, there might be a germline specific expression of VPS13A associated with the function of chorein in mesoderm differentiation.

5.6 ChAc pathology in muscle and nerve

Muscle weakness and atrophy, hyporeflexia and the elevation of serum CK are frequently present in ChAc, and suggest neuromuscular impairment in ChAc. As noted before (Aasly et al. 1999), electrophysiology demonstrates sensory axonopathy in ChAc patients. Concerning muscle pathology, both neuropathic and myopathic alterations are found. This is supported by previous studies (Limos et al. 1982; Alonso et al. 1989). Compared to MLS patients, muscle atrophy in ChAc is more severe and is marked by decreased mean fiber diameter, increased atrophy coefficients (Table 8) and a higher number of internalized nuclei in ChAc (Table 7). However, neurogenic signs like angulated fibres and muscle fibre-type grouping in ChAc are comparable to MLS (Table 7) (Hewer et al. 2007). Slight loss of myelinated fibres and axonal damage have been reported in ChAc nerve before (Sorrentino et al. 1999), while in this study, as in MLS no overt abnormalities are found.

In erythrocytes from ChAc patients the structure of band 3 complex is altered, which affects the binding of spectrin cytoskeleton to erythrocyte membranes (De et al. 2004). Therefore, the signal transduction pathways are influenced, leading to the deficiency in the process. In regard to uneven and discontinuous chorein distribution along the sarcoplasm still found, we speculate that muscle was the least influenced tissue in ChAc patients. Moreover, β -spectrin immunostaining for cytoskeletal protein is normal in the muscle of ChAc (Saiki et al. 2007). In conclusion, there might be a reasonable mechanism for this selective expression in the muscle. It is also necessary to exclude the mutated chorein, which can be expected in some cases, such as missense mutations, deletion of exons without changing the reading frame, and frameshift mutations leading to premature termination codons but not to nonsense-mediated mRNA decay.

There is a hypothesis that the impairment of chorein leads to neuroaxonal dystrophy through influencing axonal transport (Dotti et al. 2004), which possibly explained the nerve damage. However, chorein is not present in the peripheral nerves of normal control, which is different from chorein expression in brain and muscle. This finding could interestingly explain our nerve histological results. Even in case 9 with the longest duration of disease (21 years), no overt abnormalities were found in the nerve (Figure 14). Therefore, we speculate that chorein absence might not be intensively involved in the physiological processes of the peripheral nerves in ChAc, or might at least not be necessary for these processes.

5.7 Epidemiology of NA in China

Involuntary movements and orofacial dyskinesias are the most common symptoms and found in respectively 91% and 79% of Chinese NA cases. The proportion of orofacial dyskinesias in HD is reported as 13.7% (Zheng et al. 2012), which was far less than the proportion in NA. Thus, orofacial dyskinesias might be a relatively

specific symptom for the diagnosis of NA (Bader et al. 2010). Ataxia was observed and was more commonly seen in the phenotype of PKAN (Ichiba et al. 2008). 19% patients suffered from epilepsy and 26% patients had psychiatric symptoms, which is much lower than the reported proportions (50% patients with epilepsy and 2/3 patients with psychiatric symptoms) in the literatures (Scheid et al. 2009; Bader et al. 2011). We should also carefully explain the results and pay attention to the potential bias, e.g. publication bias and completeness of results. The ethnic difference might be another possible explanation.

The current clinical diagnosis of NA in China is mainly based on clinical manifestations such as hyperkinetic movement disorders and elevated proportion of acanthocytes in the blood, as well as the exclusion of other possible diseases. The diagnostic criteria for NA were widely used in the last century. There was also an early Chinese case was diagnosed in Singapore according to the criteria (Ong et al. 1989). With the development of molecular biology, the absence of acanthocytes has been found in certain gene-confirmed ChAc cases (Bayreuther et al. 2010). On the other hand, not all NA cases first present choreic movement or orofacial dyskinesias, but sometimes atypical symptoms such as epilepsy, psychiatric disorders, or parkinsonism.

In addition to ChAc, other subtypes of NA such as MLS, HDL-2 and PKAN, have not been found in China. We noticed that some cases were with young age of onset or suffered from ataxia. It is necessary to differentiate from NBIA, which is also an inherited neurological movement disorder. NBIA is usually early-onset and ataxia is more common in NBIA. Therefore, specific molecular tests are required for the accurate diagnosis. For instance, chorein detection by Western blot is a reliable and inexpensive method for ChAc diagnosis (Dobson-Stone et al. 2004). In the future, Chinese NA network is required and encouraged for the improvement of diagnosis,

treatment, care and research.

6 Outlook

This doctoral dissertation adds the knowledge to the neuropathology of ChAc and the epidemiology of NA in China. Because of the very low prevalence in the past, there were only sparse clinico-pathological case reports of ChAc. Moreover, the distribution of chorein in the human tissues was not investigated, as well as the role of chorein absence in the pathogenesis of ChAc. In the study, chorein was found widely distributed in the brain and mesoderm organs of normal control subjects. Chorein was not expressed in the normal peripheral nerves, which illustrated that chorein might not be intensively involved in the physiological processes of the peripheral nerves, or might at least not be necessary for these processes. In the future, the exact mechanisms need to be further investigated.

The conclusion in neuromuscular finding suggests that both neurogenic and myopathic alterations are involved in ChAc. It is important to the concept of diagnosis and treatment, which are different from the simple myopathy. The neuropathological changes in the striatum and hippocampus of ChAc highlight the astrogliosis and the decrease of SP projection system. These findings are different from HD. It has been reported ENK projection system in the striatum was more affected than SP in HD and related to choreiform movement disorders. The impairment of SP system might explain the early presentation of parkinsonism in certain ChAc cases. Meanwhile, there was also decrease of ENK in the striatum of ChAc, which is comparable to the striatum of HD. Elevated ENK in the hippocampus of ChAc was found, and it was similar to the changes of hippocampus in Alzheimer's disease. Therefore, we believed neurochemical changes in ChAc hippocampus also contributed to the cognitive decline, not only the striatal involvement.

The limitations of the study should be considered and need to be improved in the future. The tissues were collected worldwide, and the heterogeneity of specimens in

post mortem interval and duration of fixation was unavoidable. However, these factors are very important for immunohistochemistry. For each stain, only one section was evaluated from each block and the potential of bias might exist in the calculation of positive-stained neurons and the area of labeled boutons. Furthermore, the neurochemistry study of brain was limited to the GABAergic system, while the cholinergic system was not investigated due to the unavailability of antibodies, e.g. choline acetyltransferase and acetylcholinesterase. Therefore, the conclusions should be confirmed and supplemented by future investigations with more accurate methods. There are still some questions, which are needed to explore. Firstly, what are the functions of chorein and the mechanisms of chorein absence in the pathological changes of ChAc? Secondly, what are the associations between chorein absence and the neurochemical changes in the brain, and why the astrogliosis is more predominant in ChAc, compared with HD? Is there any correlation between chorein absence and astrogliosis? Finally, the iron depositions are reported in the neurodegenerative diseases, such as neurodegeneration with brain iron accumulation, progressive supranuclear palsy and HD. However, these diseases are associated with the pathological accumulations, which is absent in ChAc. In the preliminary study, we found sparse iron depositions in the perivascular and parenchyma of ChAc striatum and it is much less than the iron depositions in HD. The mechanisms of iron depositions in ChAc and the differences between ChAc and HD should be interestingly further investigated.

7 Summary

Chorea-acanthocytosis (ChAc) is a VPS13A gene related, rare autosomal recessive neurodegenerative disease. Chorein is a 360 kDa protein encoded by VPS13A, which is absent in the erythrocyte membrane of ChAc. Actually, ChAc is the most common phenotype of neuroacanthocytosis (NA) syndromes, which are generally acknowledged as a group of rare diseases and characterized by misshaped erythrocytes (acanthocytes) and neuronal multisystem pathology. The core symptoms include choreiform involuntary movement, muscle weakness and atrophy, areflexia, elevated creatine kinase, dementia and psychiatric disorders. Because of the low prevalence of ChAc, no study systematically evaluated the pathological changes based on the autopsy cohort.

My doctoral project consists of four studies investigating neuropathology of ChAc and epidemiology of NA syndromes in China. The first study explored the distribution of chorein in normal control with upregulated levels throughout the brain and mesoderm organs. In the second study, we examined muscle and nerve tissues of ChAc. Both neurogenic and myopathic alterations were found in the muscle histology. Cross sections of sural nerves showed no overt abnormalities. The third study focused on neuropathological changes in the ChAc brains. Astrogliosis was involved in the pathological process of ChAc and the predominant neurochemical impairment was substance P projection system, widely locating in dorsal caudate nucleus, dorsal putamen, internal segment of the globus pallidus and hippocampus. Meanwhile, the loss of enkephalin in dorsal caudate nucleus and putamen, as well as the elevation of enkephalin in hippocampus might contribute to clinical manifestation. The fourth study was an overview of NA case reports in Chinese medical database in the past 30 years. There were only 53 probable NA cases reported and none of them was confirmed by gene or protein test. In the future, the network of Chinese NA is needed for the

improvement of diagnosis, treatment, research and education.

8 Zusammenfassung

Die Chorea-Akanthozytose (ChAc) ist eine seltene autosomal-rezessive neurodegenerative Erkrankung mit Mutationen im VPS13A-Gen. Das Produkt des VPS13A-Gens ist Chorein, ein Protein 360 kDa Massengewicht. Bei ChAc-Patienten fehlt Chorein u.a. in den Erythrozytenmembranen. ChAc ist die häufigste Erkrankung innerhalb der Gruppe von Neuroakanthozytose (NA)-Syndromen. NA ist die Sammelbezeichnung für eine Gruppe von seltenen Erkrankungen, die durch die Kombination aus deformierten Erythrozyten (Akanthozyten) und multisystemischer Hirnpathologie gekennzeichnet sind. Die Hauptsymptome sind unwillkürliche choreatische Bewegungen und Muskelschwäche, ferner Areflexie, Demenz und psychiatrische Störungen. Es zeigt sich eine Muskelatrophie sowie eine Erhöhung der Kretininkinasewerte. Wegen der geringen Prävalenz von ChAc gibt es bislang keine systematische Studie über pathologische Veränderungen in Autopsiegeweben.

Mein Promotionprojekt bestand aus vier Studien, die sich v. a. auf neuropathologische Veränderungen bei ChAc und auf die Epidemiologie von NA-Syndromen in China konzentrierten. Die erste Studie untersuchte die Normalverteilung des Chorein-Proteins in Gehirn und mesodermalen Organen gesunder Kontrollfälle. Die zweite Untersuchung befasste sich mit histopathologischen Veränderungen der Skelettmuskulatur und peripherer Nerven bei ChAc. In den Muskelpräparaten wurden sowohl neurogene als auch myopathischen Veränderungen gefunden. Die Querschnitte vom Nervus suralis zeigten keine offensichtlichen Anomalien. Die dritte Untersuchung verglich die neuropathologischen Veränderungen in den Gehirnen von Fällen mit ChAc und Morbus Huntington gegenüber normalen Kontrollen. Eine Vermehrung der Astroglia (Astrogliose) war ein Bestandteil des pathologischen Prozesses bei ChAc. Am stärksten beeinträchtigt war das Substanz P-Projektionssystem im dorsalen Nucleus caudatus, dorsalen Putamen, internen

Segment des Globus pallidus und Hippocampus. Der Verlust von Enkephalin im dorsalen Nucleus caudatus und Putamen sowie die verstärkte Enkephalinexpression im Hippocampus tragen möglicherweise außerdem zur klinischen Manifestation bei. Die vierte Untersuchung war eine Übersicht der NA-Fallberichte in den letzten 30 Jahren in der chinesischen medizinischen Datenbank. Es gab lediglich 53 Fälle mit wahrscheinlicher NA, jedoch keiner dieser Fälle wurde durch Gen- oder Eiweißtests bestätigt. In Zukunft wird ein Netzwerk zur Erfassung chinesischer Fälle mit V.a. NA benötigt, um Diagnostik, Behandlung, Forschung und Ausbildung zu verbessern.

9 Appendix

Protocol of Western Blot for Chorein Distribution

1. Tissue homogenates by Lysis Buffer^A to 10% solution
2. 5ul unfrozen supernatant of homogenates, mixed with 15ul LDS Sample Buffer^B
10min. 70°C
3. Electrophoresis in Gel-Running Buffer^C (1 hour, 150V per gel)
4. Activate PVDF membrane with methanol, and equilibrate with Transfer Buffer^D
5. Transfer PVDF membrane with Transfer Buffer and 10% methanol (50mA per membrane, 2 hours)
6. Block the membrane with 0.5% I-block, PH=7.4, 1 hour Room Temperature
7. Primary antibody, anti-chorein 1 Antiserum (Rabbit) 1:5000 in PBST^E, 1 hour Room Temperature
8. Wash with PBST 4x15 min., Room Temperature
9. Secondary antibody, 1:5000 in PBST, 1 hour Room Temperature
10. Wash with PBST 4x15 min., Room Temperature
11. Equilibrate with alkaline phosphatase (AP^F) Buffer 5 min., Room Temperature
12. Develop with CDP star solution on membrane in foil and camera, about 10 mins exposure
13. Develop with NBT-BCIP^G (NBT:BCIP=35ul+45ul+10ml AP buffer)

Buffers:

- A. Lysis Buffer: 100nM Tris, 100mM NaCl, 10mM EDTA, 0.5% nonidet P40, 0.5% deoxycholic acid, 1 tablet protease-Inhibitor/10ml, PH 6.9
- B. LDS Sample Buffer: 100ul LDS, 180ul aqua dest, 20ul mercapto
- C. Gel-Running Buffer: 100ml Gel-Running Buffer 10x (50mM Tris-Base, PH8.3, 60.5g/L; 50mM Tricine 89.5 g/L; 0.1% SDS 10.0 g/L), 900ml aqua dest
- D. Transfer Buffer: 10ml Transfer Buffer 20x (Invitrogen, NU Page, Cat. no. NP

0006(11), 180ml aqua dest, 10ml methanol

- E. PBST Buffer: 100ml PBS-Buffer 10x (Na_2HPO_4 , 12.7g/L; NaH_2PO_4 3.9 g/L; NaCl 85 g/L), 900ml aqua dest, 1ml Tween-20
- F. AP Buffer: 100mM Tris-HCl (PH 9.5), 100mM NaCl and 10mM MgCl_2
- G. NBT-BCIP Substrate Solution: BCIP-T (50mg/ml in dimethylformamide) 33ul, NBT (75mg/ml in 70% dimethylformamide) 44ul, with 10ml of AP Buffer

10 Abbreviations

| | |
|-----------|--|
| AP | Alkaline phosphatase |
| A β | Amyloid-beta |
| CA | Cornu ammonis |
| CALB | Calbindin D-28k |
| Cd | Caudate nucleus |
| ChAc | Chorea-acanthocytosis/Chorea-Akanthozytose |
| CK | Creatine kinase |
| CM | Centromedian |
| CPC | Centromedian-parafascicular complex |
| CSF | Cerebrospinal fluid |
| DG | Dentate gyrus |
| e.g. | Exempli gratia |
| ENK | Enkephalin |
| etc. | Et cetera |
| EvG | Elastica-van Gieson |
| FUS | Fused in sarcoma |
| GABA | Gamma-aminobutyric acid |
| GAD | Glutamic acid decarboxylase |
| GFAP | Glial fibrillary acidic protein |
| GPe | External segment of the globus pallidus |
| GPI | Internal segment of the globus pallidus |
| GT | Gömöri trichrome |
| HD | Huntington's disease |
| HDL-2 | Huntington's disease-like 2 |
| H&E | Hematoxylin and eosin |

| | |
|------|--|
| IOD | Integrated optical density |
| KB | Klüver-Barrera |
| MBP | Myelin basic protein |
| MHC | Myosin heavy chain |
| MLS | McLeod syndrome |
| NA | Neuroakanthozytose/Neuroacanthocytosis |
| NBIA | Neurodegeneration with brain iron accumulation |
| PAS | Periodic acid Schiff |
| Pf | Parafascicular |
| PKAN | Pantothenate kinase-associated neurodegeneration |
| Pt | Putamen |
| SP | Substance P |
| SPSS | Statistical package for the social sciences |

11 References

- Aasly J, Skandsen T, Ro M (1999). Neuroacanthocytosis--the variability of presenting symptoms in two siblings. *Acta Neurol Scand* 100: 322-325.
- Alonso ME, Teixeira F, Jimenez G, Escobar A (1989). Chorea-acanthocytosis: report of a family and neuropathological study of two cases. *Can J Neurol Sci* 16: 426-431.
- Badawy RA, Lai A, Vogrin SJ, Cook MJ (2013). Subcortical epilepsy? *Neurology* 80: 1901-7.
- Bader, B, Arzberger T, Heinsen H, Dobson-Stone C, Kretzschmar HA, Danek A (2008). Neuropathology of chorea-acanthocytosis. In: Walker RH, Saiki S, Danek A (eds). *Neuroacanthocytosis Syndromes II*. Springer: Berlin Heidelberg. pp 187-195.
- Bader B, Danek A, Walker RH (2011): Chorea-acanthocytosis. In: Walker RH (ed). *The differential diagnosis of chorea*. Oxford University Press: New York. pp 122-148.
- Bader B, Walker RH, Vogel M, Prosiegel M, McIntosh J, Danek A (2010). Tongue protrusion and feeding dystonia: a hallmark of chorea-acanthocytosis. *Mov Disord* 25: 127-129.
- Bayreuther C, Borg M, Ferrero-Vacher C, Chaussenot A, Lebrun C (2010). Chorea-acanthocytosis without acanthocytes (French). *Rev Neurol* 166: 100-103.
- Beckstead RM, Kersey KS (1985). Immunohistochemical demonstration of differential substance P-, met-enkephalin-, and glutamic-acid-decarboxylase-containing cell body and axon distributions in the corpus striatum of the cat. *J Comp Neurol* 232: 481-498.
- Bo L, Li YM, Liu FH (2005). Care for one case of chorea-acanthocytosis (Chinese).

- Chin J Prac Nurs 21: 54-55.
- Bodnar RJ, Klein GE (2005). Endogenous opiates and behavior: 2004. *Peptides* 26: 2629-2711.
- Bosman GJ, Bartholomeus IG, De Grip WJ, Horstink MW (1994). Erythrocyte anion transporter and antibrain immunoreactivity in chorea-acanthocytosis. A contribution to etiology, genetics, and diagnosis. *Brain Res Bull* 33: 523-528.
- Bostantjopoulou S, Katsarou Z, Kazis A, Vadikolia C (2000). Neuroacanthocytosis presenting as parkinsonism. *Mov Disord* 15: 1271-1273.
- Brickner JH, Fuller RS (1997). SOI1 encodes a novel, conserved protein that promotes TGN-endosomal cycling of Kex2p and other membrane proteins by modulating the function of two TGN localization signals. *J Cell Biol* 139: 23-36.
- Burbaud P, Vital A, Rougier A, Bouillot S, Guehl D, Cuny E, et al. (2002). Minimal tissue damage after stimulation of the motor thalamus in a case of chorea-acanthocytosis. *Neurology* 59: 1982-1984.
- Chen W, Wang WA, Liu ZG (2008). One case of chorea-acanthocytosis and review (Chinese). *Chin J Prac Int Med* 28: 890-891.
- Cui AQ, Li YB, Liu SP, Chen YP, Li DR, Xu JL (2005). Hereditary chorea-acanthocytosis (Chinese). *Journal of Shanxi Medical University* 36: 93-95.
- Cui AQ, Li YB, Liu XX, Chen YP, Li DR, Xu JL (2004). Three cases from a family constellation of heredity chorea-acanthocytosis (Chinese). *Chin J Med Gen* 5: 421.
- Danek A, Bader B, Velayos-Baeza A, Walker RH (2012). Autosomal recessive transmission of chorea-acanthocytosis confirmed. *Acta Neuropathol* 123: 905-906.
- Danek A, Jung HH, Melone MA, Rampoldi L, Broccoli V, Walker RH (2005).

- Neuroacanthocytosis: new developments in a neglected group of dementing disorders. *J Neurol Sci* 229-230: 171-186.
- Danek A, Sheesley L, Tierney M, Uttner I, Grafman J (2004): Cognitive and neuropsychiatric findings in McLeod syndrome and in chorea-acanthocytosis. In: Danek A (ed). *Neuroacanthocytosis Syndromes*. Springer: Dordrecht. pp 95-116.
- Danek A, Walker RH (2005). Neuroacanthocytosis. *Curr Opin Neurol* 18: 386-392.
- Dayer AG, Cleaver KM, Abouantoun T, Cameron HA (2005). New GABAergic interneurons in the adult neocortex and striatum are generated from different precursors. *J Cell Biol* 168: 415-427.
- de Jong GI, Naber PA, Van der Zee EA, Thompson LT, Disterhoft JF, Luiten PG (1996). Age-related loss of calcium binding proteins in rabbit hippocampus. *Neurobiol Aging* 17: 459-465.
- De FL, Olivieri O, Corrocher R (2004). Erythrocyte aging in neurodegenerative disorders. *Cell Mol Biol* 50: 179-185.
- Do VH, Martinez CO, Martinez JL, Jr., Derrick BE (2002). Long-term potentiation in direct perforant path projections to the hippocampal CA3 region in vivo. *J Neurophysiol* 87: 669-678.
- Dobson-Stone C, Danek A, Rampoldi L, Hardie RJ, Chalmers RM, Wood NW, et al. (2002). Mutational spectrum of the CHAC gene in patients with chorea-acanthocytosis. *Eur J Hum Genet* 10: 773-781.
- Dobson-Stone C, Velayos-Baeza A, Filippone LA, Westbury S, Storch A, Erdmann T, et al. (2004). Chorein detection for the diagnosis of chorea-acanthocytosis. *Ann Neurol* 56: 299-302.
- Dobson-Stone C, Velayos-Baeza A, Jansen A, Andermann F, Dubeau F, Robert F, et al. (2005). Identification of a VPS13A founder mutation in French Canadian

- families with chorea-acanthocytosis. *Neurogenetics* 6: 151-158.
- Domaradzka-Pytel B, Majak K, Spodnik J, Olkowicz S, Turlejski K, Djavadian RL, et al. (2007). Distribution of the parvalbumin, calbindin-D28K and calretinin immunoreactivity in globus pallidus of the Brazilian short-tailed opossum (*Monodelphis domestica*). *Acta Neurobiol Exp* 67: 421-438.
- Dong GF, Bao LP, Jin N, Gong ZL, Lei ZL (1989). One case of chorea-acanthocytosis (Chinese). *Chin J Prac Int Med* 9: 310.
- Dotti M, Malandrini A, Federico A (2004): Neuromuscular findings in eight Italian families with neuroacanthocytosis. In: Danek A (ed). *Neuroacanthocytosis Syndromes*. Springer: Dordrecht. pp 127-138.
- Ferrante RJ, Kowall NW, Richardson EP, Jr. (1991). Proliferative and degenerative changes in striatal spiny neurons in Huntington's disease: a combined study using the section-Golgi method and calbindin D28k immunocytochemistry. *J Neurosci* 11: 3877-3887.
- Foglia A (2010). The acanthocyte-echinocyte differential: The example of chorea-acanthocytosis. *Swiss Med Wkly* 140:w13039.
- Gradstein L, Danek A, Grafman J, Fitzgibbon EJ (2005). Eye movements in chorea-acanthocytosis. *Invest Ophthalmol Vis Sci* 46: 1979-1987.
- Haber S, Elde R (1981). Correlation between Met-enkephalin and substance P immunoreactivity in the primate globus pallidus. *Neuroscience* 6: 1291-1297.
- Hardie RJ, Pullon HW, Harding AE, Owen JS, Pires M, Daniels GL, et al. (1991). Neuroacanthocytosis. A clinical, haematological and pathological study of 19 cases. *Brain* 114: 13-49.
- He SL, Zhang Y (1988). One case of chorea-acanthocytosis (Chinese). *J Postgrad Med* 11: 26.
- Heinsen H, Arzberger T, Schmitz C (2000). Celloidin mounting (embedding without

- infiltration) - a new, simple and reliable method for producing serial sections of high thickness through complete human brains and its application to stereological and immunohistochemical investigations. *J Chem Neuroanat* 20:49-59.
- Heinsen H, Heinsen YL (1991). Serial thick, frozen, gallocyanin-stained sections of human central nervous system. *J Histotechnol* 14:167-173
- Heinsen H, Rüb U, Gangnus D, Jungkunz G, Bauer M, Ulmar G, et al. (1996). Nerve cell loss in the thalamic centromedian-parafascicular complex in patients with Huntington's disease. *Acta Neuropathol* 91:161-168.
- Heinsen H, Strik M, Bauer M, Luther K, Ulmar G, Gangnus D, et al. (1994). Cortical and striatal neurone number in Huntington's disease. *Acta Neuropathol* 88:320-333.
- Heizmann CW, Braun K (1995): Calcium regulation by calcium-binding proteins in neurodegenerative disorders. Springer: New York.
- Hewer E, Danek A, Schoser BG, Miranda M, Reichard R, Castiglioni C, et al. (2007). McLeod myopathy revisited: more neurogenic and less benign. *Brain* 130: 3285-3296.
- Holt DJ, Herman MM, Hyde TM, Kleinman JE, Sinton CM, German DC, et al. (1999). Evidence for a deficit in cholinergic interneurons in the striatum in schizophrenia. *Neuroscience* 94: 21–31.
- Hu YH, Wang HJ, Dong S (2010). Perioperative nursing of a patient with neuroacanthocytosis (Chinese). *Chin J Nurs* 45: 413-415.
- Huerta MF, Krubitzer LA, Kaas JH (1986). Frontal eye fields defined by intracortical microstimulation in squirrel monkeys, owl monkeys, and macaque monkeys. I. Subcortical connections. *J Comp Neurol* 253: 415-439.
- Ichiba M, Nakamura M, Sano A (2008). Neuroacanthocytosis update (Japanese).

- Brain Nerve 60: 635-641.
- Jia RP, Zhao XY, Xu N, Bai XH, Zhang LJ (2012). One case of chorea-acanthocytosis syndrome and literature review (Chinese). *Clinical Focus* 27: 1913-1914.
- Jiang YP (2010). Case discussion of late-onset cerebellar ataxia (Chinese). *Chin Clin Neurosci* 18: 223-224.
- Jiang YP, Zhou Y (2008). Case discussion of generalized dystonia in children (Chinese). *Chin Clin Neurosci* 16: 562-564.
- Jimenez-Corral C, Moran-Sanchez JC, Alonso-Navarro H (2006). Neuropeptides in Alzheimer's disease (French). *Rev Neurol* 42: 354-359.
- Jung HH, Danek A, Walker RH (2011). Neuroacanthocytosis syndromes. *Orphanet J Rare Dis* 6: 68.
- Kageyama Y, Matsumoto K, Ichikawa K, Ueno S, Ichiba M, Nakamura M, et al. (2007). A new phenotype of chorea-acanthocytosis with dilated cardiomyopathy and myopathy. *Mov Disord* 22: 1669-1670.
- Kalaitzakis ME, Graeber MB, Gentleman SM, Pearce RK (2008). Striatal beta-amyloid deposition in Parkinson disease with dementia. *J Neuropathol Exp Neurol* 67: 155-161.
- Kimura M, Matsumoto N (1997). Neuronal activity in the basal ganglia. Functional implications. *Adv Neurol* 74: 111-118.
- Kreczmanski P, Heinsen H, Mantua V, Woltersdorf F, Masson T, Ulfing N, et al. (2007). Volume, neuron density and total neuron number in five subcortical regions in schizophrenia. *Brain* 130:678-692.
- Kurano Y, Nakamura M, Ichiba M, Matsuda M, Mizuno E, Kato M, et al. (2007). In vivo distribution and localization of chorein. *Biochem Biophys Res Commun* 353: 431-435.
- Kuusisto E, Parkkinen L, Alafuzoff I (2003). Morphogenesis of Lewy bodies: dissimilar

- incorporation of alpha-synuclein, ubiquitin, and p62. *J Neuropathol Exp Neurol* 62: 1241-1253.
- Lauer M, Heinsen H (1996). Cytoarchitectonics of the human nucleus accumbens. *J Hirnforsch* 37: 243-254.
- Li P, Huang R, Song W, Ji J, Burgunder JM, Wang X, et al. (2012). Deep brain stimulation of the globus pallidus internal improves symptoms of chorea-acanthocytosis. *Neurol Sci* 33: 269-274.
- Limos LC, Ohnishi A, Sakai T, Fujii N, Goto I, Kuroiwa Y (1982). "Myopathic" changes in chorea-acanthocytosis. Clinical and histopathological studies. *J Neurol Sci* 55: 49-58.
- Lin FC, Wei LJ, Shih PY (2006). Effect of levetiracetam on truncal tic in neuroacanthocytosis. *Acta Neurol Taiwan* 15: 38-42.
- Liu CY, Gao J, Yang YC, Cui LY, Wan XH, Ge CW (2005). Chorea-acanthocytosis (Chinese). *Chin J Contemp Neurol Neurosurg* 5: 175-178.
- Liu SP, Li DN, Wang SZ, Hou M, Zhao QS, Lun JH, et al. (2001). Familial neuroacanthocytosis (Chinese). *Chin J Neurol* 34: 16-18.
- Lossos A, Dobson-Stone C, Monaco AP, Soffer D, Rahamim E, Newman JP, et al. (2005). Early clinical heterogeneity in choreoacanthocytosis. *Arch Neurol* 62: 611-614.
- Luo YC, Zhao B (2005). Epilepsy-onset in chorea-acanthocytosis (Chinese). *Brain Neurol Dis J* 13: 449.
- Ma CM, Han YZ, Wang HL (2012). One case report of chorea-acanthocytosis (Chinese). *Chin J Prac Nerv Dis* 15: 96.
- Martinian L, Catarino CB, Thompson P, Sisodiya SM, Thom M (2012). Calbindin D28K expression in relation to granule cell dispersion, mossy fibre sprouting and memory impairment in hippocampal sclerosis: a surgical and post mortem

- series. *Epilepsy Res* 98: 14-24.
- Meilandt WJ, Yu GQ, Chin J, Roberson ED, Palop JJ, Wu T, et al. (2008). Enkephalin elevations contribute to neuronal and behavioral impairments in a transgenic mouse model of Alzheimer's disease. *J Neurosci* 28: 5007-5017.
- Nieto MM, Guen SL, Kieffer BL, Roques BP, Noble F (2005). Physiological control of emotion-related behaviors by endogenous enkephalins involves essentially the delta opioid receptors. *Neuroscience* 135: 305-313.
- Ong B, Devathasan G, Chong PN (1989). Choreoacanthocytosis in a Chinese patient--a case report. *Singapore Med J* 30: 506-508.
- Paine MG, Babu JR, Seibenhener ML, Wooten MW (2005). Evidence for p62 aggregate formation: role in cell survival. *FEBS Lett* 579: 5029-5034.
- Parent A, De Bellefeuille L (1983). The pallidointralaminar and pallidonigral projections in primate as studied by retrograde double-labeling method. *Brain Res* 278: 11-27.
- Peppard RF, Lu CS, Chu NS, Teal P, Martin WR, Calne DB (1990). Parkinsonism with neuroacanthocytosis. *Can J Neurol Sci* 17: 298-301.
- Qu SB, Liu LR, Sheng L, Li GL (2003). One case of Chorea-acanthocytosis (Chinese). *Chinese Journal of Medical Genetics* 20: 176.
- Rampoldi L, Danek A, Monaco AP (2002). Clinical features and molecular bases of neuroacanthocytosis. *J Mol Med (Berl)* 80: 475-491.
- Rice MW, Roberts RC, Melendez-Ferro M, Perez-Costas E (2011). Neurochemical characterization of the tree shrew dorsal striatum. *Front Neuroanat* 5: 53.
- Rinne JO, Daniel SE, Scaravilli F, Pires M, Harding AE, Marsden CD (1994). The neuropathological features of neuroacanthocytosis. *Mov Disord* 9: 297-304.
- Sa ru la B, Yuan J, Zhu RX (2007). One case of chorea-acanthocytosis (Chinese). *Inner Mongolia Med J* 39: 1010.

- Sadikot AF, Parent A, Francois C (1992). Efferent connections of the centromedian and parafascicular thalamic nuclei in the squirrel monkey: a PHA-L study of subcortical projections. *J Comp Neurol* 315:137-159.
- Sadikot AF, Rymar VV (2009). The primate centromedian-parafascicular complex: anatomical organization with a note on neuromodulation. *Brain Res Bull* 78:122-130.
- Saiki S, Sakai K, Murata KY, Saiki M, Nakanishi M, Kitagawa Y, et al. (2007). Primary skeletal muscle involvement in chorea-acanthocytosis. *Mov Disord* 22: 848-852.
- Salmon DP, Filoteo JV (2007). Neuropsychology of cortical versus subcortical dementia syndromes. *Semin Neurol* 27:7-21.
- Sapp E, Kegel KB, Aronin N, Hashikawa T, Uchiyama Y, Tohyama K, et al. (2001). Early and progressive accumulation of reactive microglia in the Huntington disease brain. *J Neuropathol Exp Neurol* 60: 161-172.
- Scheid R, Bader B, Ott DV, Merckenschlager A, Danek A (2009). Development of mesial temporal lobe epilepsy in chorea-acanthocytosis. *Neurology* 73: 1419-1422.
- Seto-Ohshima A, Emson PC, Lawson E, Mountjoy CQ, Carrasco LH (1988). Loss of matrix calcium-binding protein-containing neurons in Huntington's disease. *Lancet* 1: 1252-1255.
- Simmons DA, Casale M, Alcon B, Pham N, Narayan N, Lynch G (2007). Ferritin accumulation in dystrophic microglia is an early event in the development of Huntington's disease. *Glia* 55: 1074-1084.
- Sorrentino G, De RA, Miniello S, Nori O, Bonavita V (1999). Late appearance of acanthocytes during the course of chorea-acanthocytosis. *J Neurol Sci* 163: 175-178.

- Stanley DP, Shetty AK (2004). Aging in the rat hippocampus is associated with widespread reductions in the number of glutamate decarboxylase-67 positive interneurons but not interneuron degeneration. *J Neurochem* 89: 204-216.
- Steiner J, Mawrin C, Ziegeler A, Biela H, Ullrich O, Bernstein HG, et al. (2006). Distribution of HLA-DR-positive microglia in schizophrenia reflects impaired cerebral lateralization. *Acta Neuropathol* 112: 305-316.
- Storey E, Beal MF (1993). Neurochemical substrates of rigidity and chorea in Huntington's disease. *Brain* 116: 1201-1222.
- Sun HT (2000). Two cases of chorea-acanthocytosis (Chinese). *Chin J Neurol* 33: 134.
- Tang X (2012). One case of neuroacanthocytosis (Chinese). *Chin Gen Pract* 2009 12: 2062.
- Velayos-Baeza A, Levecque C, Dobson-Stone C, Monaco AP (2008): The function of chorein. In: Walker RH (ed). *Neuroacanthocytosis Syndromes II*. Springer: Berlin Heidelberg. pp 87-105.
- Velayos-Baeza A, Vettori A, Copley RR, Dobson-Stone C, Monaco AP (2004). Analysis of the human VPS13 gene family. *Genomics* 84: 536-549.
- Kefalopoulou Z, Zrinzo L, Aviles-Olmos I, Bhatia K, Jarman P, Jahanshahi M, et al. (2013). Deep brain stimulation as a treatment for chorea-acanthocytosis. *J Neurol* 260: 303-305.
- Vital A, Bouillot S, Burbaud P, Ferrer X, Vital C (2002). Chorea-acanthocytosis: neuropathology of brain and peripheral nerve. *Clin Neuropathol* 21: 77-81.
- Walker RH, Jung HH, Danek A (2011). Neuroacanthocytosis. *Handb Clin Neurol* 100: 141-151.
- Walker RH, Velayos-Baeza A, Bader B, Danek A, Saiki S (2012). Mutation in the CHAC gene in a family of autosomal dominant chorea-acanthocytosis.

- Neurology 79: 198-199.
- Walterfang M, Evans A, Looi JC, Jung HH, Danek A, Walker RH, et al. (2011). The neuropsychiatry of neuroacanthocytosis syndromes. *Neurosci Biobehav Rev* 35: 1275-1283.
- Walterfang M, Yucel M, Walker R, Evans A, Bader B, Ng A, et al. (2008). Adolescent obsessive compulsive disorder heralding chorea-acanthocytosis. *Mov Disord* 23: 422-425.
- Wang ZM, Cao YY (2005). One case of neuroacanthocytosis, misdiagnosed as obsessive compulsive disorder (Chinese). *Chin J Psychiatry* 38: 26.
- Wei YP, Wan XH, Gao J, Gao S, Du H, Li BH, et al. (2005). The clinical and neuropathological study of three neuroacanthocytosis cases (Chinese). *Chin J Neurol* 38: 712-713.
- Weibel ER (1979). *Stereological methods*, vol 1. Academic Press: London New York. pp1-415.
- West MJ, Slomianka L, Gundersen HJ (1991). Unbiased stereological estimation of the total number of neurons in the subdivisions of the rat hippocampus using the optical fractionator. *Anat Rec* 231: 482-497.
- Xuereb JH, Perry RH, Candy JM, Perry EK, Marshall E, Bonham JR (1991). Nerve cell loss in the thalamus in Alzheimer's disease and Parkinson's disease. *Brain* 114:1363-1380.
- Yang AY, Liang YQ (1990). One case report of chorea-acanthocytosis (Chinese). *Medic J Indust Enterpr* 1: 48.
- Yang RM, Bao YZ, Chen WD (1984). Two cases of chorea-acanthocytosis (Chinese). *New Chinese Medicine* 15: 28-29.
- Yang RM, Chen WD, Lou ZP (1987). A family constellation of chorea-acanthocytosis (Chinese). *Chin J Nerv Mental Dis* 5: 311-312.

- Yang RM, Yu XE, Li K, Hou HX (2004). One case of chorea-acanthocytosis and review (Chinese). *Chin Clin Neurosci* 12: 290-293.
- Yenari MA, Minami M, Sun GH, Meier TJ, Kunis DM, McLaughlin JR, et al. (2001). Calbindin d28k overexpression protects striatal neurons from transient focal cerebral ischemia. *Stroke* 32: 1028-1035.
- Zeng GX (2006). One case of neuroacanthocytosis and review (Chinese). *Chin J Diffic Complica Case* 5: 220.
- Zhang AL, Zhao XY (2011). Chorea-acanthocytosis: a clinical report of two cases (Chinese). *Chin J Neuromed* 10: 73-75.
- Zhang JB, Gong LM, Dai JC, Han H (1989). Report of two chorea-acanthocytosis cases (Chinese). *Harbin Medical University Bulletin* 23: 285.
- Zhang QY, Wang YG, Jiang YP, Wu JJ, Feng M, Wu ZZ, et al. (2012). Neuroacanthocytosis: Report of three cases (Chinese). *Chin Clin Neurosci* 20: 18-23.
- Zhang WX, Li JR, Yang SL, Zhang XZ, An YH, Chen HZ (2003). Case report of chorea-acanthocytosis (Chinese). *Chin J Neurol* 36: 331.
- Zhao H, Mao SP (2007). Neuroacanthocytosis: Report of one case (Chinese). *Stroke Nerv Dis* 14: 318-319.
- Zhao H, Wang C, Niu FN (2012). One case of chorea-acanthocytosis and literature review (Chinese). *Chin J Diffic Complica Case* 11: 63-64.
- Zheng BR, Han H, Qi ZZ, Wang DS (1989). A case report of chorea-acanthocytosis (Chinese). *Harbin Medical University Bulletin* 23: 126-127.
- Zheng Z, Burgunder JM, Shang H, Guo X (2012). Huntington's like conditions in China, A review of published Chinese cases. *PLoS Curr* 4: RRN1302.
- Zhou H, Zhang XH, Sun YL (2007). Chorea-acanthocytosis: Reports of two cases (Chinese). *Chin J Neuroimmun Neurol* 14: 297-299.

Zhou XQ, Gua HZ, Shi XS, Cui LY, Chen L, Han YH, et al. (2012). Clinical, laboratory and neuroimaging characteristics of neuroacanthocytosis (Chinese). *Chin J Neurol* 45: 112-115.

12 Acknowledgement

This study was completed at the Department of Neurology, Klinikum Großhadern, Ludwig-Maximilians-Universität Munich and funded by the project of the European Multidisciplinary Initiative on Neuroacanthocytosis, funded by the Bundesministerium für Bildung und Forschung, Bonn Germany (project no. 01GM1003). I was funded by the state PhD scholarship from Chinese Scholarship Council.

First of all, I would like to thank Prof. Dr. med. Adrian Danek for his support and supervision of this study. In addition, I thank Dr. med. Thomas Arzberger, Center for Neuropathology and Prion Research, Ludwig-Maximilians-Universität Munich; Dr. med. Benedikt Bader and Prof. Dr. med. Benedikt Schoser, Department of Neurology, Ludwig-Maximilians-Universität Munich; Prof. Dr. med. Helmut Heinsen, Laboratory of Morphological Brain Research, Department of Psychiatry, University of Wuerzburg and Prof. Dr. med. Christoph Schmitz, Anatomy, Ludwig-Maximilians-Universität Munich for slices examination and dissertation correction, as well as Dr. Verena Hoffmann, Institute for Medical Informatics, Biometry and Epidemiology, Ludwig-Maximilians-Universität Munich for her professional guide in the statistics.

Meantime, I would like to thank Gertrud Kwiatkowski, Iryna Pigur, Michael K. Schmidt, Maren Kiessling, Jens Müller-Starck, Beate Aschauer, Ursula Klutzny, and Maria Schmuck for their technical assistance. And I am much indebted to the patients and their families and the Advocacy for Neuroacanthocytosis Patients.

I also thank to the colleagues in the University International Office and Department of Neurology, Ludwig-Maximilians-Universität Munich for their introduction to German and help in daily life.

Finally, I am very thankful for the endless support and understanding from my parents. I am deeply grateful to my grandfather for raising me up and the education from childhood. My family has been always the motivation for me.